Scaling studies of percolation phenomena in systems of dimensionality two to seven: Cluster numbers

Hisao Nakanishi*† and H. Eugene Stanley
Department of Physics and Center for Polymer Studies, Boston University, Boston, Massachusetts 02215
(Received 27 December 1979)

Cluster statistics are obtained by computer simulation for percolation processes on d-dimensional lattices with $d=2$ through 7. For all d, n_s, the number of s-site clusters per site, is found to satisfy reasonably well the scaling hypothesis first proposed by Stauffer. The scaling functions are analyzed for dimensional dependence, and it is found that as d increases they approach very rapidly the exactly known result for the Bethe lattice corresponding to $d=\infty$. Corrections to scaling are also studied, and at the upper critical dimension $d_c=6$, a deviation from scaling consistent with a logarithmic correction is obtained. Some universal quantities such as the ratio of the amplitudes C_+ and C_- of the "susceptibility" (second moment of n_s) below and above the percolation threshold p_c are also found to approach the Bethe lattice limit very quickly. In addition, our data suggest that C_+/C_- already assumes the limiting value of unity for $d=6$. This is consistent with the exact relation for the asymmetric decay of n_s proved by Kunz and Souillard if we adopt the hypothesis that the asymmetry of n_s about p_c only enters the corrections to the leading scaling term for $d \geq 6$.

I. INTRODUCTION

The study of critical phenomena has seen remarkable progress, largely due to the concept of scaling[1] and to the renormalization-group (RG) approach[2] that stems from it. Thus, after the connection was established between percolation and other critical phenomena by Kasteleyn and Fortuin[3] a number of studies have been made to understand scaling in percolation.[4] One approach has been to exploit fully the correspondence between percolation and q-state Potts model in the limit $q \to 1$ and to study the scaling of the analog of the thermodynamic equation of state.[5] Another approach is to focus attention directly on the scaling of the cluster size distribution function n_s.[6] In this paper, we shall discuss only the latter approach; a second paper dealing with the equation of state in d-dimensional percolation will be published elsewhere.

Although the past work illuminates many aspects of scaling, a number of important questions remain unanswered. For example, the universality classes for percolation were not fully explored since no numerical study of the global features of the scaling functions was made for systems of dimensionality greater than three. In particular, the onset of mean-field-like behavior as d increases past the upper critical dimension $d_c=6$ was not treated numerically in the context of scaling previously.[7] One related question is how to reconcile the symmetric mean field scaling function with the asymmetry that arises from the theorem of Kunz and Souillard.[8] Moreover, corrections to scaling have been analyzed numerically only in two dimensions; in particular, detailed Monte Carlo work is available only for the site problem on the triangular lattice.[6] In the following sections we address these and other questions, drawing our data from extensive Monte Carlo simulations for $d=2, 3, \ldots, 7$. Our present work should be compared with those of the field-theoretic studies of Ref. 9.

This paper is organized as follows: In the remainder of this section, the scaling hypothesis[6] for n_s is restated. Section II addresses the question of the validity of this hypothesis by presenting the general features of the scaled data for n_s, while Sec. III discusses scaling and corrections to scaling at the percolation threshold p_c. Section IV is devoted to the behavior of n_s away from p_c and in Sec. V, we study the critical exponents and universal constants such as C_+/C_-. Brief conclusions are presented in Sec. VI.

In bond (site) percolation on a given lattice, bonds (sites) are occupied or empty with probability p and $(1-p)$, respectively, independent of one another. Two (occupied) sites belong to the same cluster if they are connected through occupied bonds (sites). Let n_s be the mean number of clusters containing s sites, normalized by the total number of lattice sites and taken to the thermodynamic limit. We begin by restating the hypothesis of n_s scaling as the statement that $n_s(p) \equiv n(\epsilon, y)$ is "asymptotically" [as $\epsilon \equiv (p_c-p)/p_c \to 0$ and $y \equiv 1/s \to 0$] a generalized homogeneous function (GHF)[10]; i.e., there exist two numbers a_y and a_n [a_ϵ having been fixed to $1/(2-\alpha)$ Ref. 5] such that the functional equation,

$$n(\lambda^{a_\epsilon}\epsilon, \lambda^{a_y} y) = \lambda^{a_n} n(\epsilon, y) \tag{1.1a}$$

is satisfied for all λ, ϵ, and y provided that all arguments—both sides of Eq. (1.1a)—are small. By setting $\lambda^{a_y} y = 1$, or $\lambda = y^{-1/a_y}$, we obtain

$$n(\epsilon, y) = y^{a_n/a_y} n(\epsilon y^{-a_\epsilon/a_y}, 1) \ , \tag{1.1b}$$

which can be rewritten as

$$n_s(p) = s^{-\tau} f(\epsilon s^{\sigma}) \tag{1.2}$$

with $\tau \equiv a_n/a_y$ and $\sigma \equiv a_\epsilon/a_y$.

Equation (1.2) is the n_s scaling hypothesis of Stauffer. The exponents τ and σ are related to the usual percolation exponents α, β, γ, and δ by[4]

$$\begin{aligned} &2-\alpha = (\tau-1)\sigma, \quad \beta = (\tau-2)/\sigma \ , \\ &\gamma = (3-\tau)/\sigma, \quad \delta = 1/(2-\tau) \ , \end{aligned} \tag{1.3a}$$

or

$$\tau = 2 + 1/\delta, \quad \sigma = 1/\beta\delta = 1/(\beta+\gamma) \ . \tag{1.3b}$$

With $a_\epsilon = 1/(2-\alpha)$, this leads to the identification of the scaling powers a_y and a_n,

$$a_y = a_\epsilon/\sigma = 1/(1+1/\delta), \quad a_n = \tau a_y = a_y + 1 \ . \tag{1.4}$$

II. SCALING FUNCTIONS IN d-DIMENSIONS

When Eq. (1.2) holds, we call the function $f(x)$ a scaling function. In the case of one dimension, $f(x)$ can be calculated exactly[11] as

$$f(x) = x^2 \exp(-x) \ . \tag{2.1}$$

Since $f(0) = 0$ we cannot divide $f(x)$ by $f(0)$ to normalize its amplitude unlike for $d > 1$. Therefore, we normalize $f(x)$ by dividing by its maximum value (taken at $x_{\max} = 2$) to obtain the "universal scaling function" f_1 for $d = 1$. Below we shall compare f_1 and f_d similarly defined by $d > 1$.

A second exactly solved system is the Bethe lattice of coordination number z[12] for which n_s (site problem) is given by

$$n_s = p^s q^{2+(z-2)s} z[s(z-1)]!/\{s![s(z-2)+2]!\} \ . \tag{2.2}$$

For $s \gg 1$ and $\epsilon \ll 1$, we have

$$\begin{aligned} n_s \sim\ & z[2\pi(z-2)(z-1)^3]^{-1/2} s^{-5/2} \\ & \times \exp\{-(\epsilon s^{1/2})^2 (z-1)/[2(z-2)]\} \ . \end{aligned} \tag{2.3}$$

Therefore, $f(x)$ is a Gaussian function

$$f(x) = A(z) \exp[-B(z) x^2] \ , \tag{2.4a}$$

where

$$\epsilon = (p_c - p)/p_c = 1 - (z-1)p$$

and

$$\begin{aligned} A(z) &= z[2\pi(z-2)(z-1)^3]^{-1/2} \ , \\ B(z) &= (z-1)/[2(z-2)] \ . \end{aligned} \tag{2.4b}$$

The maximum of $f(x)$ occurs at $x_{\max} = 0$, and f is symmetric about $x = 0$: $B(z)$ is a slowly varying function of z for large z with $\lim_{z\to\infty} B(z) = \frac{1}{2}$. Hence we shall write (valid also for the bond problem)

$$f_\infty(x) = \exp(-\tfrac{1}{2}x^2) \ . \tag{2.5}$$

We note here that a simplified universality law, in which the normalization of the scaling variable is accomplished by the choice of $x = \epsilon s^{\sigma}$, is only valid approximately since $B(z)$ does depend (weakly) on z. In this paper, however, we shall assume this procedure to be applicable in obtaining the scaling functions f_d. For $d = 2$ and 3, as well as in the case of the Bethe lattice, there is sufficient evidence to believe its approximate validity.[6]

Figure 1 shows the shape of the scaling functions in the two limiting dimensions, $d = 1$ and ∞. Thus, we are led naturally to investigate their behavior in intermediate dimensions, particularly to find out how the $d = \infty$ limit is approached as d increases past d_c.

In all dimensions, $n_s(p)$ for fixed s has a single maximum as a function of p: for small p, it clearly

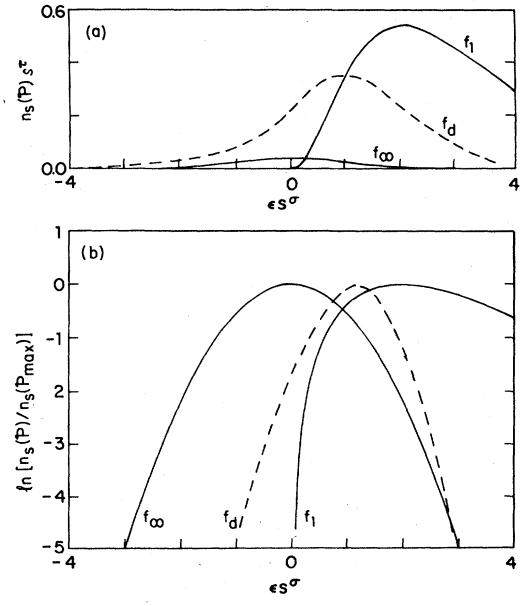

FIG. 1. Universal scaling functions f_1 and f_∞ for $d = 1$ and the Bethe lattice ($Z = 14$), respectively. A linear scale is used in (a), and in (b) the curves are obtained by first dividing by the maximum value and then plotting them using a semilog scale. The broken curves schematically represent a scaling function for $1 < d < \infty$.

increases with p while, as p becomes large, most sites are annexed by very large clusters thereby "draining" n_s for a given s. Thus, defining $p_{\max}$ to be the maximum for n_s, we can fit a straight line to the log-log plot of $(p_c - p_{\max})$ vs s in accordance with the scaling law (1.2). In practice, there is a question of what value to use for p_c since its effective value p_c^{eff} for a finite lattice may be quite different from the true p_c. One way to resolve this question self-consistently is to vary the trial value of p_c^{eff} until the best linearity is achieved (as evidenced in the correlation coefficient R being closest to unity). This procedure was followed in two and three dimensions where $p_{\max}$ can be estimated fairly accurately, whereas in $d > 4$, where scarcity of data and the broadness of the peaks of n_s curves prevent us from locating $p_{\max}$ with any accuracy, we simply use the series estimates of p_c as p_c^{eff}.

In two dimensions, we obtain in this way $p_c^{\text{eff}} = 0.50115$ for the bond problem on the square lattice (where $p_c = 0.5$ exactly), and the fitted line gives

$$(p_c^{\text{eff}} - p_{\max}) s^{0.400 \pm 0.010} = 0.458 \pm 0.03 \ , \qquad (2.6a)$$

with $R = 0.99934$, in fair agreement with the series estimate[13] of σ of about 0.389. (This fit was achieved over the range $2^5 \leq s < 2^{15}$. For the details of the actual Monte Carlo realizations, we refer the reader to Appendix A.) If the true value of p_c is used instead, the resulting exponent becomes about 0.43, a little too large, and R drops to 0.99905. For $d = 3$, the corresponding equation for the cubic bond problem is

$$(p_c^{\text{eff}} - p_{\max}) s^{0.504 \pm 0.030} = 0.203 \pm 0.03 \ , \qquad (2.6b)$$

where the choice of $p_c^{\text{eff}} = 0.2498$ was made. If the series estimate[14] 0.247 of the true p_c is used instead, the exponent corresponding to σ becomes 0.74, much larger than the series estimate[14] of 0.48, and R is also low at 0.98825. The value $x_{\max}$ of the scaling variable for which $f(x)$ takes its maximum is approximately 0.9 in two dimensions and 0.8 in three dimensions. This is in contrast to Hoshen *et al.*,[6] which found $x_{\max}$ to be about 0.8 for both $d = 2$ and $d = 3$.

For the reasons cited above, for $d = 4$ and 5, the linear fit to the log-log plot of $(p_c^{\text{eff}} - p_{\max})$ vs s is merely an order of magnitude estimate. With this in mind, we give below the best fits using the series estimates[15] of p_c, 0.197 for $d = 4$ and 0.141 for $d = 5$, in place of p_c^{eff}. For the hypercubic site problem in $d = 4$, it is

$$(p_c - p_{\max}) s^{0.46} = 0.077 \ , \qquad (2.6c)$$

with $R = 0.99005$. Similarly, for the hypercubic site problem in $d = 5$, we obtain

$$(p_c - p_{\max}) s^{0.57} = 0.048 \ , \qquad (2.6d)$$

in rather poor agreement with the combined series–Monte Carlo estimate[7,15] of $\sigma = 0.52$. The data for $p_{\max}(s)$ for $d = 2$ through 5 are plotted in Fig. 2 along with the best fits given in Eqs. (2.6), and the location $x_{\max}$ and value $n_s(p_{\max})/n_s(p)$ of the maxima of $f(x)$ are summarized in Table I.

For $d \leq 5$, $p_{\max}(s)$ for all s studied is smaller than the estimate of p_c made from susceptibility [by shifting the trial value of p_c^{eff} until the exponents γ (below p_c) and γ' (above p_c) match]. For $d = 2$, p_c according to this method is about 0.5035 for 1000 × 1000 samples (square-bond problem); for $d = 3$

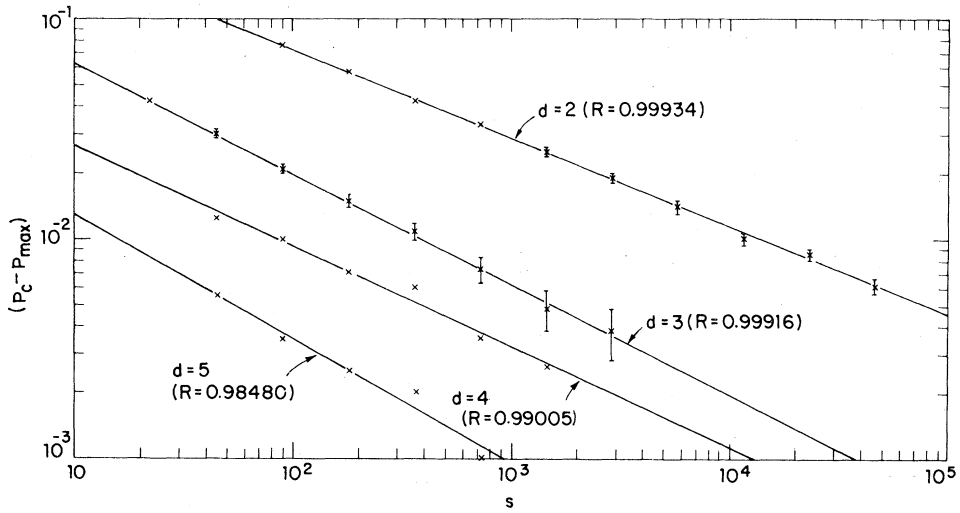

FIG. 2. Test of scaling for the maxima of n_s curves for $d = 2$, 3, 4, and 5. The error bars included for $d = 2$ and 3 are those associated with finding $p_{\max}$ on the n_s curves, not including the errors in each point on these same curves.

TABLE I. Dimensional dependence of the location (x_{max}) and value $[n_s(p_{max})/n_s(p_c)]$ of the maximum of the scaling function $f(x)$, normalized by its value at p_c.

d	x_{max}	$[n_s(p_{max})/n_s(p_c)]$
1	2	∞
2	0.8 – 0.9	4.8
3	0.6 – 0.8	1.6
4	0.4 – 0.45	1.4
5	0.35 – 0.4	1.1
6	. . . [a]	1.0
7	. . . [a]	1.0
∞	0	1

[a]Our data suggest values significantly larger than 0; however, there are reasons to believe they are spurious. See text.

(cubic-bond problem), 4 and 5 (hypercubic-site problems), it is 0.252, 0.198, and 0.143, respectively. For the hypercubic site problem in six dimensions, where samples containing one million sites are used, we obtain $p_c = 0.108$ in this way. For this dimension, however, the peaks occur clearly on both sides of $p = 0.108$ [cf. Fig. 3(a)]. In addition, for large s, p_{max} appears to be almost constant at about 0.110. We interpret this as the further shift of p_c^{eff} and that the s dependence of p_{max} derives from the corrections to scaling (perhaps higher corrections than the leading logarithmic modulation). This conclusion is supported both by a good overall data collapse and the studies of a smaller system (the reader is referred to Appendix A for details).

In seven dimensions, where 8^7 (> two million) site samples are used, the peaks of the n_s curves [cf. Fig. 3(b)] are too broad to admit any reasonable estimates. Therefore, no attempt is made to plot $(p_c - p_{max})$ against s. However, a feature clearly different from all previous data ($d \leq 6$) is observed. That is, for small s, p_{max} is clearly above p_c (which is estimated to be 0.085 from susceptibility, in fair agreement with the $1/z$ expansion of Gaunt *et al.*[15]), and as s grows, the peaks move closer to p_c. In other words, the peaks move toward smaller p as s increases, in contrast to $d \leq 6$ where the opposite occurs (discussions in Appendix A). We also note, as in $d = 6$, p_{max} for large s appears to be stationary at about 0.085. Our interpretation here is similar to that in $d = 6$; the scaling term makes only symmetric contribution with $p_{max} = p_c = \text{const}$.

On the other hand, we may investigate the entire scaling function $f(x)$ by plotting $n_s(p)/n_s(p_c)$ for various values of p and s, thus checking whether the data points collapse onto a single curve. In two dimensions, this is done using the true p_c of 0.5 and the series estimate 0.389 of σ while in three dimensions, the value 0.250 close to the p_c^{eff} estimated in (2.6b) is used together with $\sigma = 0.47$, a combined series–Monte Carlo estimate.[7,14] For $d = 4$ and 5, we use the series estimates[15] for p_c^{eff}, and the series–Monte Carlo estimates[7,15] for σ. In six and seven dimensions, σ is known exactly to be the mean-field value of 0.5, and for p_c^{eff}, we use 0.110 for $d = 6$ [cf. Fig. 3(a)] and 0.085 for $d = 7$ [cf. Fig. 3(b)]. The scaled data thus obtained are plotted in Fig. 4(a)–4(f).

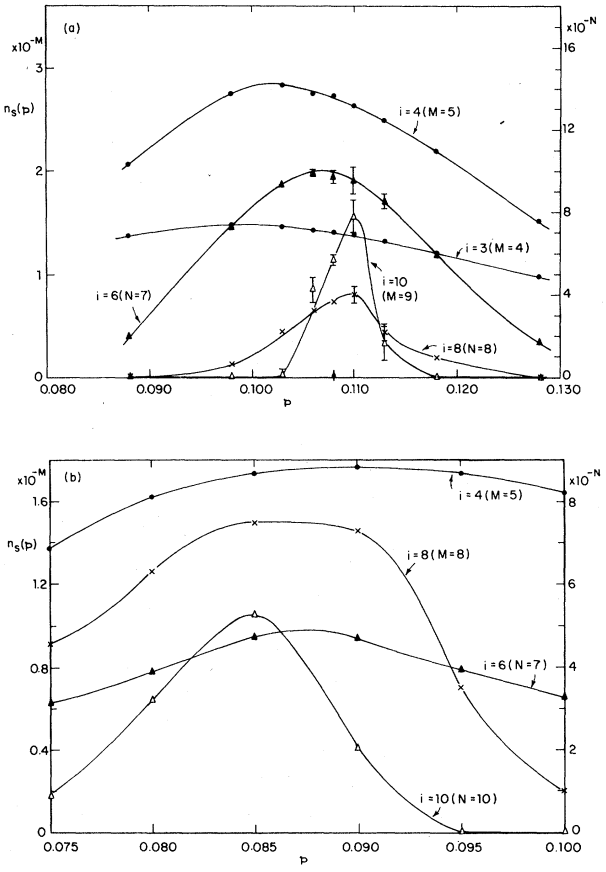

FIG. 3. The cluster size distribution n_s is plotted for fixed values of s as function of p for (a) $d = 6$, and (b) $d = 7$. The error bars in (a) are the standard deviations obtained by separating the total sample into three groups of 10 realizations each. The values i indicate the bins $2^i \leq s < 2^{i+1}$.

For $d = 2$, data collapsing is seen in a rather wide range of p and s, in complete agreement with the previous results.[5,6] In the neighborhood of $x = 0$, the scaling function is nearly linear, and when plotted against $(p_c - p)s^{\sigma}$, its slope is about 7.5 ± 0.2, again in agreement with the previous result from the triangular site problem.[6] This slope enters an expression for the mean perimeter-to-volume ratio for a cluster of size s as explained by Stauffer.[4] For $d = 3$, 4, and 5, its value is 5.5 ± 0.4, 4.7 ± 0.4, and

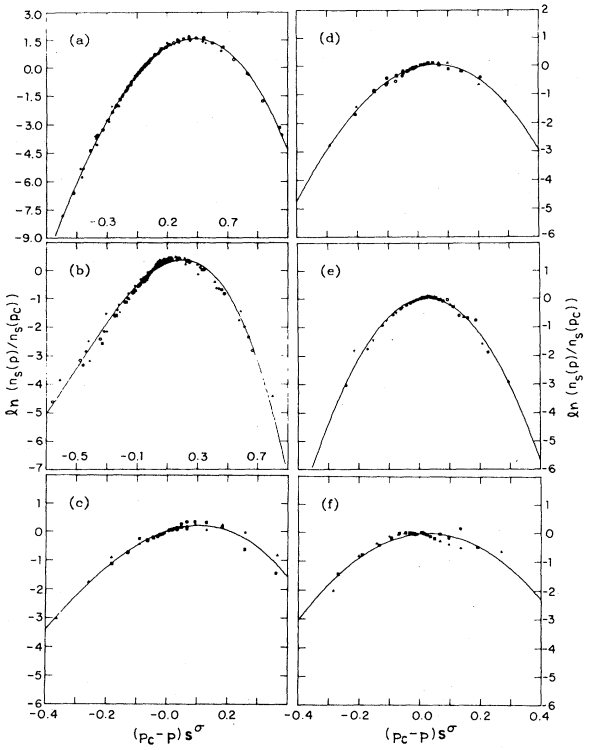

FIG. 4. The scaled data for n_s in (a) $d=2$ to (f) $d=7$ together with the least-squares fits (for $d=2$ to 5, cubic polynomials are fitted, for $d=6$ and 7, quadratic ones are used).

3.9 ± 0.4, respectively. In six dimensions it is about 4.4, but in view of our interpretation that the asymmetric appearance of Fig. 4(e) results from the correction terms to scaling [and that therefore Fig. 4(e) does not accurately represent the scaling function], this number may not have much physical meaning. In the seven-dimensional case, the scaling function of Fig. 4(f) is extremely flat, even flatter than f_∞ (if plotted with proper normalization), so that it does not allow an estimate of $x_{\max}$ or the slope at $x=0$. However, it does seem clear that, if f_∞ (Fig. 1) is indeed the universal scaling function for $d=\infty$, then the case for $d=7$ has moved somewhat "past" it. The peculiar behavior of the peaks of n_s curves mentioned above corroborates this impression. Whether or not this is a real trend that continues to even higher dimensions is unclear, and it will be of interest to study at what d, if at all, the scaling function "turns around."

In summary, we have shown in this section that the general trend established in $d=2$ and 3 continues to achieve a rapid convergence toward f_∞ except that in $d=7$, this trend appears to "overshoot" in some respects. There does not seem to be any indication of irregularity at $d=4$, as predicted in Ref. 16; i.e., the percolation fixed point found in $(6-d)$ expansion is stable to ϕ^4 perturbation, although the ϕ^4 operator becomes relevant below $d=4$ with respect to the Gaussian fixed point.

III. SCALING AND CORRECTIONS TO SCALING AT p_c

Scaling law (1.2) reduces at p_c to

$$n_s(p_c) = s^{-\tau} f(0) \equiv q_0 s^{-\tau} \ . \tag{3.1}$$

Therefore, neglecting corrections, a log-log plot of n_s vs s should yield a straight line for sufficiently large s. Indeed this behavior was found previously in $d=2$ (triangular site[6] and square site[17]) and $d=3$ (simple cubic and bcc 1, 2 site[6]) over 5 to 6 decades of s.

Assuming (3.1), the amplitude q_0 can be estimated theoretically in at least two ways (Ref. 4 and references therein). First, we note

$$\sum_s s n_s = 1 (\text{or } p) \text{ for } p \leq p_c \tag{3.2a}$$

in bond (or site) problem, and that

$$\sum_s s n_s(p_c) = q_0 \sum_s s^{1-\tau} = q_0 \zeta(1+1/\delta) \ , \tag{3.2b}$$

where $\tau = 2 + 1/\delta$ and $\zeta(x) \equiv \sum i^{-x}$ (Riemann zeta function) have been used. Thus,

$$q_0 = 1/\zeta(1+/\delta) \quad [\text{or } p_c/\zeta(1+1/\delta)] \tag{3.3}$$

and the estimates using this are tabulated in Table II. Since this method requires only the knowledge of p_c and δ in addition to a good table of the zeta function, it is very convenient to use to estimate q_0 in all dimensions. However, we observe that q_0 (or q_0/p_c in site problem) would have to be a universal quantity according to (3.3) while, e.g., $n_1(p_c) = (1-p_c)^z$ [or $n_1(p_c)/p_c$ in site problem], where z is the coordination number of the lattice, is certainly not universal although it may assume fairly close values for different lattices (also between site and bond problems) of the same dimensionality. For example, the bond problem on the simple cubic lattice gives $n_1(p) = 0.18$ while the fcc bond problem yields 0.22, and the diamond lattice bond problem gives 0.14.[18] This means that the degree of departure from scaling (3.1) of n_s for small s greatly differs from lattice to lattice—and for some lattices, (3.1) is optimally satisfied. This is in fact the case for the square-bond problem as seen below.

The second method consists of the following. Eq. (55) of Ref. 6 gives

$$q_0 = E/[\delta\Gamma(1-1/\delta)] \quad \{\text{or } p_c E/[\delta(1-1/\delta)]\} \ , \tag{3.4}$$

where E is the amplitude in the scaling relation $P(p_c, H) = EH^{1/\delta}$ and $\Gamma(x)$ is the gamma function. Since E is estimated for various lattices in $d=2$ and 3

TABLE II. Estimates of the amplitude of the scaling function from Eqs. (3.3) and (3.4). The estimate of δ is obtained by the combination of the series and Monte Carlo results. The values of the Riemann zeta function are computed approximately by interpolating from those given in Jahnke, Emde, and Lösch (Ref. 35).

d	δ	$\Gamma(1-1/\delta)$	E	$q_0(q_0/p_c)$ Eq. (3.4)	$\tau(1+1/\delta)$	$q_0(q_0/p_c)$ Eq. (3.3)
1	∞	1	1	0	∞	0
2	18.0	1.04	1.1[a]	0.056	18.5	0.054
3	5.3	1.15	1.31–1.38[a]	0.22	5.8	0.17
4	3.9	1.24	· · ·	· · ·	4.6	0.22
5	3.0	1.37	· · ·	· · ·	3.6	0.28
≥ 6	2	1.77	· · ·	· · ·	2.612	0.38

[a]Reference 19.

by series expansion methods,[19] this can also be a suitable method to obtain q_0. Similar comments as above apply here also, and in particular, if Eq. (3.1) held rigorously, then q_0 (or q_0/p_c in site problem) would be universal, and thus E would also be universal. The series results for E indeed point to near universality, which is a corroborating evidence for the goodness of the approximation in Eq. (3.1). These estimates are shown in Table II.

In addition, Ref. 6 estimated the correction to Eq. (3.1) in the triangular site problem assuming a general form for $x=\epsilon s^{\sigma}$ and a suitable exponent Ω,

$$n_s = s^{-\tau} f(x) - s^{-\tau-\Omega} f_1(x) + \cdots , \tag{3.5a}$$

which reduces at $\epsilon = 0$ to

$$n_s = q_0 s^{-\tau}(1 - X s^{-\Omega} + \cdots) . \tag{3.5b}$$

In scaling approach, one only needs to include one other scaling field μ (an "irrelevant" one) in n_s in addition to ϵ and $y = 1/s$ to obtain Eq. (3.5). Thus, (1.1a) becomes

$$n(\lambda^{a_\epsilon}\epsilon, \lambda^{a_y} y, \lambda^{a_\mu}\mu) = \lambda^{a_n} n(\epsilon, y, \mu) \tag{3.6a}$$

and the analog of Eq. (1.1b) is now given by

$$n(\epsilon, y, \mu) = y^{a_n/a_y} n(\epsilon y^{-a_\epsilon/a_y}, 1, \mu y^{-a_\mu/a_y}) . \tag{3.6b}$$

Therefore, we have for the scaling law,

$$n_s(\epsilon, \mu) = s^{-\tau} g(\epsilon s^{\sigma}, \mu s^{a_\mu/a_y}) . \tag{3.7a}$$

Suppose g can be expanded in powers of μ,[20]

$$n_s(\epsilon, \mu) = s^{-\tau} g(\epsilon s^{\sigma}, 0) + \mu s^{-\tau+a_\mu/a_y} g_1(\epsilon s^{\sigma}, 0) + \cdots , \tag{3.7b}$$

which leads in $\epsilon \to 0$ limit to

$$n_s \sim q_0 s^{-\tau}(1 + q_1 s^{a_\mu/a_y} + \cdots) . \tag{3.8}$$

We note that, if $a_\mu > 0$, (3.7) describes a crossover (with the crossover exponent $\phi = a_\mu/a_y$), while, if $a_\mu < 0$, it describes a correction to scaling as in Eq. (3.5) which is small for large s.

In the language of RG, this means that, if μ is a relevant operator, there is a crossover and that, if μ is irrelevant, there is a correction to scaling.[20] Assuming that we have no other relevant operator to consider here, we choose for μ the most important irrelevant operator, namely, the one with the least negative a_μ. At $d=6$, we must consider the problem separately since there exists a marginal operator μ with $a_\mu = 0$ (the ϕ^3 operator in the field-theoretic language[16]). Thus, the size of this crossover term is a function of two factors: how far a given system is located from the fixed point [reflected in the constant amplitude in (3.8)] and how fast the fixed point is approached in the μ direction as the RG is repeatedly applied (a_μ/a_y). This is an important fact, and we will come back to it shortly.

To relate this "correction" exponent a_μ/a_y to other familiar ones, first note that the analog of the free energy in percolation is the mean number of clusters. To be precise,

$$G(\epsilon, H) = \sum_s n_s(\epsilon) \exp(-Hs) \tag{3.9}$$

corresponds to the $q \to 1$ limit of the free energy of the q-state Potts model with the dimensionless exchange integral J [where $p = 1 - \exp(-J)$] and the dimensionless external magnetic field H. The scaling

assumption (1.1) for n_s then implies

$$G_{\text{sing}}(\lambda^{a_\epsilon}\epsilon, \lambda^{a_y}H) = \left(\sum_s \exp(-\lambda^{a_y}Hs)\, n(\lambda^{a_\epsilon}\epsilon, y)\right)_{\text{sing}} = \left(\sum_s \exp[-H(\lambda^{a_y}s)]\, n(\lambda^{a_\epsilon}\epsilon, \lambda^{a_y}/(\lambda^{a_y}s))\right)_{\text{sing}}$$

$$= \lambda^{-a_y}\left(\sum_{s'} \exp(-Hs')\, n(\lambda^{a_\epsilon}\epsilon, \lambda^{a_y}/s')\right)_{\text{sing}} = \lambda^{a_n - a_y} G_{\text{sing}}(\epsilon, H) \ , \tag{3.10}$$

which means

$$a_n - a_y = 1, \quad a_y = a_h \ . \tag{3.11}$$

Note a_ϵ, a_y, and a_n were defined so that the scaling law $G_{\text{sing}}(\lambda^{a_\epsilon}\epsilon, \lambda^{a_h}H) = \lambda G_{\text{sing}}(\epsilon, H)$ holds in the first place. Thus,

$$-a_\mu/a_y = -a_\mu/a_h = -da_\mu/da_h \ , \tag{3.12a}$$

where $-da_\mu$ is the so-called "correction-to-scaling exponent" usually denoted by ω. Moreover,

$$da_h = d/(1+1/\delta) \ , \tag{3.12b}$$

or using the hyperscaling law $d\nu = 2 - \alpha$ (valid only for $d \leq 6$),

$$da_h = \beta\delta/\nu \ , \tag{3.12c}$$

giving

$$\Omega = -a_\mu/a_y = \omega\nu/\beta\delta \tag{3.13}$$

[or $\omega(1+1/\delta)/d$ for $d > 6$]. A table summarizing these exponents estimated from a field-theoretic RG on the Potts model[21] (ω) and the series and Monte Carlo methods[7,14,15] (β, δ) is produced below (Table III). Note that, since the Gaussian fixed point is stable to the perturbation of ϕ^3 operator above $d = 6$, the result $\omega = \frac{1}{2}(d-6)$ is exact for $d > 6$.

Equations (3.8) and (3.13) together, then, give the scaling law with the leading correction to be tested (for $d \neq 6$) by computer simulations. On the other hand, as we obtained these by scaling ϵ, we could also scale y. In that case, the scaling law to be tested would be

$$n_s(\epsilon, \mu) = \epsilon^{\tau/\sigma}\hat{g}(y\epsilon^{-1/\sigma}, 0) + \mu\epsilon^{\tau/\sigma - a_\mu/a_\epsilon}\hat{g}_\cdot(y\epsilon^{-1/\sigma}, 0) + \cdots \ , \tag{3.14}$$

and as $s \to \infty$,

$$n_s \sim \epsilon^{\tau/\sigma}(1 + \text{const}\ \epsilon^{-a_\mu/a_\epsilon} + \cdots) \tag{3.15a}$$

with

$$-a_\mu/a_\epsilon = \omega\nu \ . \tag{3.15b}$$

As mentioned above, $d = 6$ is a special case. In the case of a thermal n-vector model, the ϕ^4 operator [which is irrelevant at the Wilson-Fisher fixed point in $(4-d)$ expansion] becomes marginal at $d = 4$, inducing logarithmic corrections to various thermodynamic functions.[22] In the present case of percolation, the ϕ^3 operator plays a similar role and introduces logarithmic corrections to the percolation analogs of these functions (mean number of clusters, percolation probability, and mean size of finite clusters, etc.).[9] We show in Appendix B, a logarithmic

TABLE III. The correction-to-scaling exponent ω and the corresponding correction exponent Ω for n_s. The exponent ω is from the $(6-d)$ expansion with resummation, and β and γ are from the combined estimates using both the series and Monte Carlo results.

d	ω	ν [$= (2\beta+\gamma)/d$ for $d \leq 6$]	$\omega\nu$	Ω ($= \omega\nu/\beta\delta$ for $d \leq 6$)
1	...	1	...	...
2	1.11[a]	1.36	1.50	0.59
3	1.01[a]	0.85	0.86	0.40
4	0.85[a]	0.64	0.54	0.27
5	0.59[a]	0.52	0.31	0.16
6	0	0.5	0	0
7	0.5	0.5	0.25	0.11
d	$\frac{1}{2}(d-6)$	0.5	$\frac{1}{4}(d-6)$	$\frac{3}{4}(d-6)$
∞	∞	0.5	∞	0.75

[a]Reference 21.

correction for n_s given by

$$n_s \sim s^{-2.5}(\ln s)^{\theta} , \tag{3.16}$$

where $\theta = \frac{2}{7}$ exactly from the $(6-d)$ expansion.

In Figs. 5(a)–5(f), curves of $n_s(p)$ vs s are shown on a log-log scale. Fig. 5(a) for the square bond problem in $d=2$ and Fig. 5(b) for the simple cubic bond problem may be compared with the similar results of Ref. 6 for the triangular site problem in $d=2$ and the simple cubic and bcc 1,2 site problems in $d=3$. However, for $d=2$, one immediately notices a striking difference; namely, Fig. 5(a) is considerably more linear. This is borne out also in the plot (not shown) of $n_s s^{\tau}$ against $\ln s$ (with the series estimate[19] 2.05 for $\tau = 2 + 1/\delta$). Almost constant, the latter figure implies the smallness of the correction-to-scaling amplitude compared to its counterpart in the triangular-site problem.

When we try to fit a straight line to Fig. 5(a) we find that the slope varies from 1.97 to 2.10 depending on the range of s to be fitted. This is of course partly due to the statistical fluctuations and finite size effects (in particular, the oscillatory behavior for very large s), but also to the systematic corrections induced by the largest irrelevant operator [cf. Eq. (3.8)]. To estimate the relative correction amplitude q_1 and exponent Ω, we plot in Fig. 6(a) $s^{\tau} n_s$ against s^{-x} for trial values of x. Since in the bond problem we get a one site cluster as a minimal cluster (when all bonds surrounding a site are empty) as opposed to the site problem where the minimal size is zero, the data point corresponding to $s=1$ can be safely discarded for the scaling analysis. We also note that the data for $s \geq 512$ corresponds to the region of large systematic increase in $s^{\tau} n_s$ corresponding to the finite size effects (not shown). Thus, we consider the region $2 \leq s < 512$ for the purpose of studying the correction to scaling, keeping in mind that a slight finite-size effect would be sufficient to mask it. When we consider this region of Fig. 6(a) only, we have a clear indication that Ω is somewhere between 0.6 and 1.0 (and closer to 0.6). This compares well with the finding of Ref. 6, that $\Omega \cong 0.67$ and with

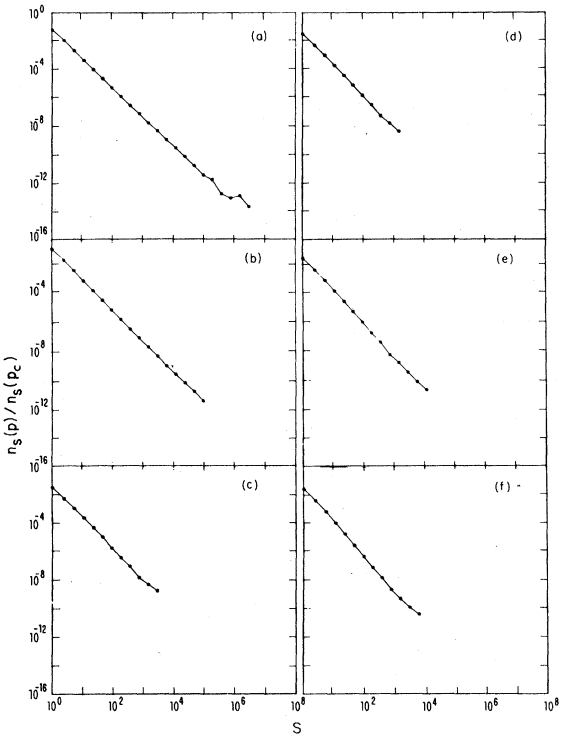

FIG. 5. Cluster size distribution at p_c in (a) $d=2$ to (f) $d=7$. For $d=2$, $(2000)^2$ samples are used for this plot. The line segments merely connect the data points.

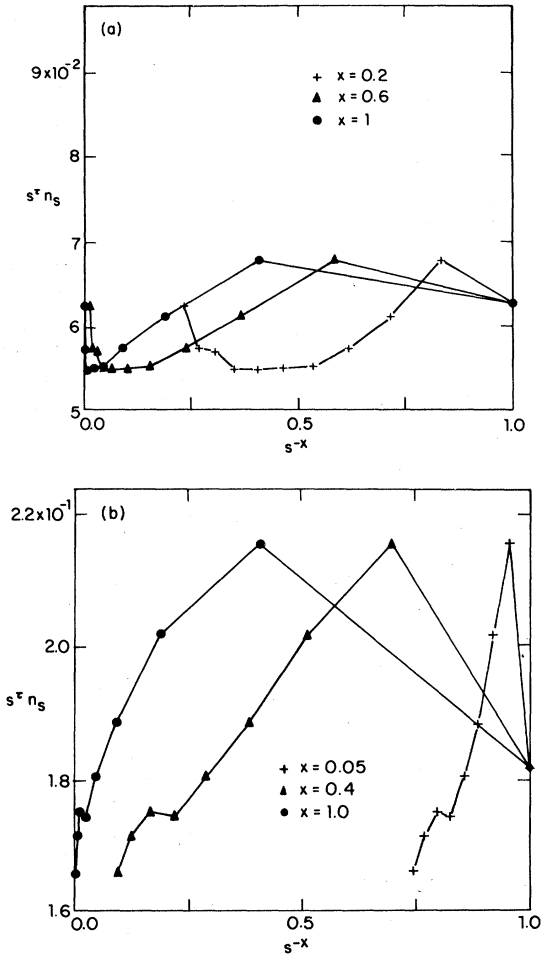

FIG. 6. Correction to scaling are estimated by plotting $s^{\tau} n_s(p_c)$ vs s^{-x} for various trial values of x. (a) is for $d=2$ [45 samples of $(1000)^2$ square lattice for $0.499 \leq p \leq 0.501$ are used]; + for $x=0.2$, Δ for 0.6, and ● for 1. (b) is for $d=3$, + for $x=0.05$, Δ for 0.4, and ● for 1.0.

the $(6-d)$-expansion result (with resummation) listed in Table III, thus demonstrating universality for the correction exponent Ω.

If we assume $\Omega \cong 0.6$ in order to estimate the amplitude C of the correction term, then $C \cong 0.029$. The scaling amplitude q_0, on the other hand, is about 0.062 directly estimated from the least-squares fit to our data, while the value obtained by using E estimated by series expansion[19] [cf. Eq. (3.4)] is 0.056 as shown in Table II. Thus, the relative amplitude of the correction term to the scaling term $q_1 = C/q_0$ is about 0.45. We note that the corresponding amplitude for the triangular site problem[6] of -1.19 is (1) negative, and (2) more than twice as large in magnitude. Therefore, we demonstrate the nonuniversality of the correction amplitude relative to the scaling term. This is as it should be since Eq. (3.7b) clearly states that this amplitude is proportional to μ, a nonuniversal quantity which measures the distance of the system at (ϵ, μ) from the fixed point. However, we note that if $n_s \sim q_0 s^{-\tau}(1+q_1 s^{-\Omega})$ held exactly, then $P(p_c, H) = EH^{1/\delta}(1 - FH^{\Omega})$ would also be exact with $E = \delta q_0 \Gamma(1-1/\delta)$ and $F = -q_1 \Gamma(1-1/\delta-\Omega)/[(1+\delta\Omega)\Gamma(1-1/\delta)]$. This would mean that if F were universal, then q_1 would also be universal. Gaunt and Sykes[19] found F to be close to universal for two dimensions in contrast to our data which indicate that q_1 varies a great deal from lattice to lattice.

For $d \geq 3$, p_c is not exactly known and τ not as accurately estimated as in $d=2$ (except for $d \geq 6$ where τ is 2.5 exactly). Nevertheless, we carry out the same sort of analysis basically for the reason that τ is known sufficiently accurately that the correction exponent Ω (as read from Table III) should be much larger than the uncertainty in τ. We would also like to know simply whether the best estimates for these exponents are consistent with one another. For the details of the Monte Carlo realizations, the reader is referred to Appendix B.

For $d=3$, we see a remarkably straight line in Fig. 5(b) with the fitted exponent varying from 2.16 to 2.24 and amplitude from 0.16 to 0.22 depending on the range covered by the least-squares fit. From the graph of $s^{\tau} n_s$ (with $\tau = 2.19$ from Table III), we can see perhaps the range $2 \leq s < 512$ would be suitable to analyze correction from, and in this region Fig. 6(b) indicates a reasonable estimate of $\Omega = 0.4$, in agreement with Table III. The relative amplitude can also be obtained from the same figure, giving $C/q_0 = 0.08/0.16 = 0.5$, with the sign of the correction term again positive. We note that a simple linear fit to Fig. 5(b) in this range yields $\tau = 2.24$ and amplitude $= 0.22$, while q_0 estimated from Eq. (3.3) should be about 0.17 and from Eq. (3.4) about 0.22. With an estimate of q_1 for the simple cubic-site problem, we would be able to consider whether a bond problem is in general "closer" to scaling than a site problem. There is some evidence that this is true in the two dimensional square lattice. Unfortunately, Ref. 6 does not discuss corrections to scaling in $d=3$.

For $d=4$ and 5, we have fewer and less accurate data than other dimensions, and thus the correction-to-scaling analysis is rather difficult. In the case of the four-dimensional hypercubic-site problem, a linear fit to Fig. 5(c) ranges in slope from 2.15 to 2.30 and in amplitude from 0.034 to 0.063 depending on the range of s covered by the fit. These numbers should be compared with the combined series-Monte Carlo estimate[7,15] of 2.26 for τ, and with 0.043 for q_0 from Eq. (3.3). Focusing our attention on relatively small s, we can see that $\Omega \cong 0.2$ would not be inconsistent with the data (cf. Table III) while $q_1 \cong -0.6$ is a very rough estimate. At any rate, it seems likely that the correction term is negative, as in the triangular site problem but opposite to both the square- and simple cubic-bond problems. The linear fit to Fig. 5(d) for the five-dimensional hypercubic-site problem yields slope between 2.21 and 2.26, and amplitude between 0.033 and 0.039 depending on the range. The series-Monte Carlo estimate[7,15] for τ is 2.33 while the estimate of q_0 from Eq. (3.3) is 0.039. It seems that $0.16 < \Omega < 0.5$, and $q_1 \cong -0.54$, again a negative correction term. We also note that, using the Eq. (3.3) estimates for q_0, the amplitude E can be estimated to be about 1.04 in $d=4$ and 1.11 in $d=5$.

For $d=6$, excepting the last two points ($s > 1024$), a linear fit seems rather good, which yields $\tau = 2.38$ and amplitude $= 0.042$ for the hypercubic site problem. The estimate of q_0 from Eq. (3.3) gives 0.042 while the Bethe lattice solution with $z=12$ yields 0.041. Here, we know τ to be exactly 2.5, and therefore, we expect to find the correction term more reliable. We also have much better statistics than for $d=4$ or 5.

Noting the region $2 \leq s < 1024$ of Fig. 7, we attempt to test a logarithmic correction as mentioned

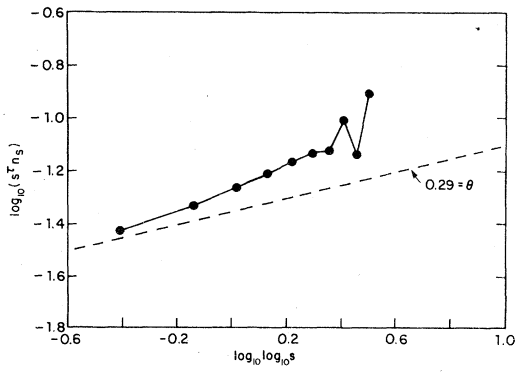

FIG. 7. Test of logarithmic correction for the six-dimensional hypercubic site problem. Plotted are $s^{\tau} n_s$ vs $\log_{10} s$ on a log-log scale. The broken line has a slope of 0.29, the theoretical prediction for the exponent of the $\ln s$ term.

before [cf. Eq. (3.16)]. Figure 7 seems to indicate fairly well a correction close to a logarithmic one with $\theta \cong 0.45$. In view of the fact that in Sec. V we see an p_c^{eff} of 0.108 from the susceptibility, we have also studied similar figures for $p = 0.108$. The conclusion remains the same except now θ appears to be about 0.56. These values are not very close to the theoretical prediction of $\frac{2}{7} = 0.29$, and we attribute this to: (1) probably p_c^{eff} of 0.110 being a slight underestimate, and (2) insufficient statistics and finite size preventing us from going further into the asymptotic region.

For $d = 7$, we use samples of the hypercubic lattice of size 8^7. Although this is a rather large lattice in terms of the volume (more than two million sites), the smallness of the linear dimension is quite restrictive. Figure 5(f) shows $n_s(p = 0.085)$ against s. A linear fit to this plot yields a slope between 2.35 and 2.49, and amplitude between 0.024 and 0.035. The zeta-function estimate of the amplitude is 0.033 while the Bethe lattice solution with $z = 14$ gives 0.034. Since τ is exactly known for all $d \geq 6$ to be 2.5, this perhaps restricts the amplitude to be that associated with the slope of 2.49 or about 0.035. Figure 5(f) shows severe finite-size effects, and therefore we do not attempt to estimate correction to scaling. However, a plot similar to Fig. 6 appears to show a very small correction-to-scaling amplitude (not shown). Noting that the finite-size effects scale as $1^{-1/\nu}$,[23] and that $\nu = 0.5$ for $d \geq 6$, it appears as if samples as large as 10^7 sites would be needed before we can attempt such a task, as we needed 10^6 sites for the case of $d = 6$.

Thus, both scaling and correction-to-scaling analyses yield striking confirmation of Stauffer's hypothesis and other previous calculations, except in the analysis of the size of the correction term F. Universal and nonuniversal quantities are clearly distinguished, and first numerical estimates of some of these are obtained. We observe a rapid convergence toward the result for the Bethe lattice in the sense that scaling amplitudes approach the Bethe lattice result very fast. A correction consistent with a logarithm is for the first time proposed and observed for $d = 6$.

IV. CLUSTER NUMBERS AWAY FROM p_c

Various power laws described so far are "critical" power laws in the sense that they follow from scaling (or GHF) hypotheses near the percolation threshold. There are other power laws that are valid away from p_c that do not appear to follow from usual scaling. In this section, we discuss these and their interplay with the critical power laws.

Kunz and Souillard[8] proved the asymptotic relations for fixed p and $s \to \infty$, in d dimensions,

$$\ln n_s \sim \begin{cases} -as^{1-1/d} & \text{for } p \geq p_1 (> p_c), \quad (4.1a) \\ -bs & \text{for } p \leq p_2 (< p_c), \quad (4.1b) \end{cases}$$

for suitable choices of p_1 and p_2. This gives a rigorous foundation for the exponent ζ proposed by Bakri and Stauffer,[24]

$$\ln n_s \sim -s^{\zeta} \quad \text{as } s \to \infty \ . \quad (4.2)$$

As is clear from Eq. (4.2), this is a law governing the asymptotic decay of the cluster number with the discrepancy between ζ and unity describing its departure from the pure exponential decay. As opposed to power law behavior at p_c, it describes behavior away from the critical threshold.

Equations (4.1) have been tested numerically in two dimensions in a few studies. In particular, Hoshen *et al.*[6] state that, in their Monte Carlo data for the triangular site problem, p_2 can be as large as 0.47 and p_1 as small as 0.505. In fact, Klein and Stauffer[25] recently presented a RG argument that these decay laws must be valid all the way up to p_c (excluding p_c itself, of course). We shall see later on in this section, however, that our Monte Carlo data do not necessarily support this argument.

Now, recall from Eq. (2.7b) that n_s can be written as

$$n_s = s^{-\tau} f(\epsilon s^{\sigma}) + s^{-\Omega-\tau} f_1(\epsilon s^{\sigma}) + \cdots \ , \quad (4.3)$$

where the effects of the irrelevant fields are taken into account in the scaling approach. In the limit $\epsilon \to 0$, $s \to \infty$ with $\epsilon s^{\sigma} \to$ const, the first term clearly dominates; this is the asymptotic scaling region. In contrast, the limit used in the decay law (4.1) or (4.2) is for fixed $\epsilon (\neq 0)$ and $s \to \infty$ implying $\epsilon s^{\sigma} \to \infty$. Since GHF hypotheses such as Eq. (1.1a) require small arguments throughout (corresponding to the closeness to criticality), this latter limit may even make (4.3) no longer valid. However, because the inclusion of more and more correction terms presumably enlarges the region of applicability of the scaling hypothesis, we shall assume (4.3) to be valid for fairly large values of ϵs^{σ} for the sake of the ensuing argument. Then the question is whether the first term in Eq. (4.3) continues to dominate in this limit or the correction terms become more important. Recall we have seen in Eq. (3.7b) that these correction terms are the derivatives of the "scaling" function with respect to composite variables containing irrelevant fields [such as μ in Eq. (3.7)]. This implies that neither of the two possibilities can be excluded from the general consideration of scaling alone. Consider, e.g., $g(x,y) = \exp(-x^2 + x^2 y)$ and $h(x,y) = \exp[-x^2 + y\exp(-x^2)]$. Then, $y(\partial g/\partial y)_{y=0} = x^2 y \exp(-x^2)$, whereas $y(\partial h/\partial y)_{y=0} = y\exp(-2x^2)$. If one has $y \sim s^{-\Omega}$ and $x \sim s^{\sigma}$ (with $2\sigma > \Omega$), then $g(x,0) = h(x,0) = \exp(-x^2)$ decays for large s more

rapidly than $y(\partial g/\partial y)_{y=0}$ but more slowly than $y(\partial h/\partial y)_{y=0}$.

However, we may consider the consequences of making either assumption, and examine them against our Monte Carlo data. Thus, suppose the scaling term dominates in the limit of fixed ϵ and $s \to \infty$ in Eq. (4.3). Then, provided that ϵ is within the range of applicability of Eq. (4.1), we must have

$$\ln f(\epsilon s^{\sigma}) \cong \ln[n_s/n_s(\epsilon=0)]$$

$$\cong \begin{cases} -a(\epsilon)s^{1-1/d} + \bar{a}(\epsilon,s) \text{ for } p > p_c & (4.4a) \\ -b(\epsilon)s + \bar{b}(\epsilon,s) \text{ for } p < p_c \ , & (4.4b) \end{cases}$$

where $\bar{a}$ and $\bar{b}$ contain weaker s-dependences than s^{ζ}. Although this leads to fractional powers of $x = \epsilon s^{\sigma}$ on the right-hand sides of Eqs. (4.4), and thus seems to give rise to the nonanalyticity of f as a function of x, the apparent singularity at $x = 0$ is of no concern since Eqs. (4.4) are considered here only in the limit $x \to \infty$. Thus, it follows that

$$a(\epsilon) = a_0 \epsilon^{(1-1/d)\sigma} \text{ for } p > p_c \quad (4.5a)$$

$$= b_0 \epsilon^{1/\sigma} \text{ for } p < p_c \ , \quad (4.5b)$$

where a_0 and b_0 are constants. We note that the $\ln(s)$ term arising from $s^{-\tau}$ has already been factored out. Also, in order to make numerical fits feasible, we shall assume $\bar{a}$ and $\bar{b}$ to be independent of s. This, of course, leads to $\bar{a} = \bar{a}_0 = \text{const}$ and $\bar{b} = \bar{b}_0 = \text{const}$ since $\bar{a}$ and $\bar{b}$ must be functions of ϵs^{σ}.

Thus, we have derived power laws for the Kunz-Souillard decay amplitudes assuming the dominance of the scaling term in Eq. (4.3). Clearly, the converse is also true; if Eq. (4.5) holds, then the dominant term can be cast into a scaling form. We must emphasize, however, that scaling does not *a priori* determine whether or not the first term dominates. Although some numerical studies related to Eq. (4.5b) do exist in $d = 2$,[26] this crucial point was not recognized previously. In fact, within rather large uncertainties, our results suggest some sort of a crossover from two and three dimensions, where Eq. (4.5) is valid, to seven dimensions, where it is probably not.

In this context, we should note that the scaling dominance (4.4) requires asymmetry of $f(\epsilon s^{\sigma})$, and thus the asymmetry of susceptibility $\chi = \sum_s s^2 n_s = \sum_s s^{2-\tau} f(\epsilon s^{\sigma})$ about $\epsilon = 0$. This would, of course, mean $C_+/C_- \neq 1$; however, $C_+/C_- \neq 1$ does not necessarily imply the dominance of the scaling term because both terms could be asymmetric with only the correction term giving the dominant Kunz-Souillard asymmetry. C_+/C_- will be studied in detail in Sec. V, and the result, in short, is that it decreases monotonically from about 200 in $d = 2$ to probably 1 in $d = 6$ (not clear in $d = 7$). If we assume in addition that C_+/C_- remains unity for all $d > 6$, then the scaling function cannot dominate in Eq. (4.3) for any finite $d > 6$.

We note that the Bethe lattice scaling function does obey Eqs. (4.4) and (4.5) since $\sigma(d=\infty) = \frac{1}{2}$, $\ln(f_\infty) \sim -\epsilon^2 s$ (both above and below p_c) while $1 - 1/d \to 1$ as $d \to \infty$.[27] In one dimension also, $\ln(f_1) \sim -\epsilon s$ and $\sigma(d=1) = 1$ are consistent with Eqs. (4.4) and (4.5).

In studying our data, among the questions we must concern ourselves with are: (1) How close to p_c does the validity of the Kunz-Souillard law extend? (2) Are we observing the true asymptotic behavior? (3) Are fluctuations and finite size effects sufficiently small? With this in mind we study Eqs. (4.1) and (4.5). However, we shall focus on Eq. (4.5) in this section, referring the reader to Appendix C for the studies of Eq. (4.1) themselves and the associated details of the Monte Carlo realizations.

For $d = 2$, Eqs. (4.5) are studied by plotting $a(\epsilon)$ vs ϵ in a log-log plot [Fig. 8(a)]. Each data point is obtained by least-squares fitting $-\ln[n_s/n_s(p=0.5)]$ vs s by a linear function assuming $\bar{a} \cong \bar{a}_0$ as described before. This figure yields a striking linearity ($R = 0.99973$ for $p > p_c$, and $R = 0.99798$ for $p < p_c$). The slope yields 1.33 for $p > p_c$ whereas $(1 - 1/d)/\sigma$ is about 1.28 using $\sigma = 0.39$. For $p < p_c$, the slope is 2.58 to be compared with $1/\sigma = \beta + \delta \cong 2.57$ in $d = 2$. Thus, we demonstrate the dominance of the scaling term in the Bakri-Stauffer limit for both $p > p_c$ and $p < p_c$. The assumption of $\bar{a} = \bar{a}_0$ is also justified fairly well, since for $p > p_c$, $\bar{a}_0$ from these fits are between 0.16 and 0.22 throughout most of the region where Eq. (4.1) seems to be valid ($0.54 \leq p \leq 0.7$). For $p < p_c$, this value is between 2.0 and 2.5 throughout most of the range of p used ($0.275 \leq p \leq 0.495$).

For $d = 3$, the slopes can be extracted over $p \geq 0.26$ vs $s^{2/3}$ (for $p > p_c$), and they are plotted in Fig. 8(b), to be compared with Eq. (4.5a). The best linear fit gives the slope of 1.60, and since $(1 - 1/d)/\sigma$ is about 1.42 for $d = 3$, the agreement is reasonable. The term $\bar{a}_0$ is also about constant at 0.3. For $p < p_c$, the linear fits against s are much better than those against $s^{2/3}$ in the case of $p > p_c$, and the region where these fits are unquestionably better is also larger, extending at least from 0.23 to 0.20 all with $R > 0.999$. Fig. 8(b) also demonstrates Eq. (4.5b) by yielding a slope of 2.21 whereas $1/\sigma$ is about 2.13 for $d = 3$. The value $\bar{b}_0$ appears to be between 0.7 and 1.0 justifying our assumption of $\bar{b}_0 = \text{const}$ as before.

In Figs. 8(c) and 8(d), we have the slopes from linear fits against $s^{1-1/d}$ for $p > p_c$ [cf. (4.4a)] and against s for $p < p_c$ [cf. (4.4b)] plotted as functions of $|p_c - p|$ for $4 \leq d \leq 7$. Since we have only 2 or 3 data points for each d (except for $d = 6$ where we have more, and for $d = 7$ where we have only a single point below p_c), whatever slope we extract from

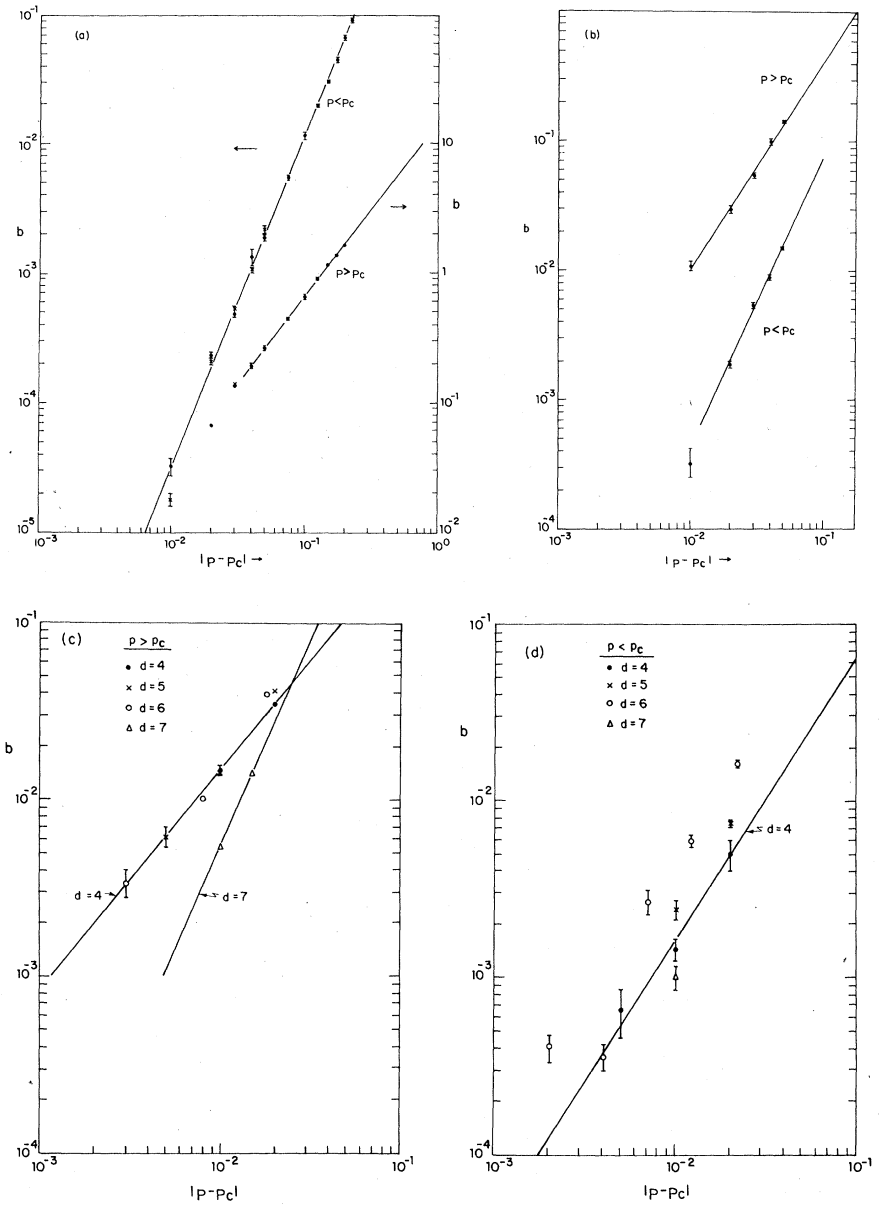

FIG. 8. Test of the dominance of the scaling term in Eq. (4.3) in Kunz-Souillard limit. The estimates for a and b [cf. (4.5)] are plotted vs $|p-p_c|$, (a) for $d=2$, (b) for $d=3$, and (c) (for $p>p_c$), (d) (for $p<p_c$) for $d=4$ through 7.

these log-log plots is bound to be a crude estimate. Nevertheless, these values may serve to throw some light upon our discussions of Eqs. (4.5) since these are the only numerical estimates available to date on this point.

In $d=4$, the slope from Figs. 8(c) and 8(d) are about 1.25 and 1.6 for $p>p_c$ and $p<p_c$, respectively, whereas $(1-1/d)/\sigma$ and $1/\sigma$ for $d=4$ would be 1.52 and 2.03, respectively. The corresponding numbers in $d=5$ are about 1.5 and 1.63 from Figs. 8(c) amd 8(d) whereas Eq. (4.5) would predict 1.55 and 1.94, respectively. Considering the scarcity of data points and the fact that each of them is secondary data themselves (estimated as slopes of least-squares fits on primary data, i.e., the cluster number), these values are certainly not incompatible with one another. The error bars shown in Fig. 8 (and in other figures) are nominal ones that follow from the least-squares fitting process, and there are in fact much larger error bars arising from the statistical errors associated with each primary data point. The total errors are not estimated because of the dif-

ficulty of weighing each data point. In $d=6$, however, we have three points for $p > p_c$ and five points for $p < p_c$ as well as the fact that each of these points is of higher accuracy. The slopes from Figs. 8(c) and 8(d) are about 1.5 and 1.7, and since $(1-1/d)/\sigma$ and $1/\sigma$ would give 1.67 and 2.0, again these numbers are inconclusive in determining if Eqs. (4.5) are valid. Finally, in $d=7$, studying $p > p_c$ only, we obtain a slope of 2.33 from Fig. 8(c) whereas $(1-1/d)/\sigma$ is exactly $12/7 = 1.71\ldots$. This discrepancy is by far the largest of all we have seen, and thus, though not conclusive, we are inclined to interpret it as indicating the breakdown of Eq. (4.5a). In fact, both at $p=0.095$ and 0.1, the linear fits against s are just as good as against $s^{6/7}$, and if indeed the decay law is $\ln n_s \sim -s$, then the above discrepancy can be understood.

Thus, our tentative conclusion is that for $d=2$ and 3, the scaling term dominates in Eq. (4.3); for $d=4$, 5, and 6, the same may or may not be true: and for $d=7$, the correction terms are likely to be the more important part in the limit of fixed ϵ and $s \to \infty$.

V. CRITICAL EXPONENTS AND UNIVERSAL CONSTANTS

In this section, we discuss some of the universal constants. Most familiar among them are the critical exponents. In particular, the percolation probability $P \sim |\epsilon|^{\beta}$ determines β while the mean cluster size $S \sim |\epsilon|^{-\gamma}$ defines the exponent γ. However, since in the simulations finite size effects often shift the location of apparent singularity away from the true p_c, we are faced with a choice of how to calculate these exponents. If the true value of p_c happens to be known (either exactly or else with very high accuracy by an independent method such as series expansions), we may use such a value and then obtain the exponents by simply power-law fitting the data. An alternative is to somehow estimate p_c^{eff} consistent with the particular function of interest as well as with the particular samples (type and size) as we have already seen in earlier sections. In studying the susceptibility, we opt for this latter approach since there exists a particularly simple method of estimating p_c^{eff} for this function; that is, we adjust trial values of p_c^{eff} so that γ matches γ' as was done in Ref. 6. This method differs from that we used previously for the same two-dimensional Monte Carlo data, and thus it yields somewhat different values for the exponents from those reported before.[5] In those dimensions for which we do not have too many values of p, this gives a very convenient method to define effective p_c and thus to compute the exponents. Of course, for the percolation probability, which is nonzero only for $p > p_c$ in the infinite lattice limit, this method cannot be used. In such cases, we find it most convenient to first determine what range of $p\,(>p_c)$ to study and then to shift the trial value of p_c^{eff} until the best fit to a power law is achieved (as evidenced by the correlation coefficient closest to unity). Table IV summa-

TABLE IV. Critical exponents β, γ and the universal susceptibility amplitude ratio C_+/C_- for $d=2$ through 7. The last column gives γ/β (with β and γ being either exact or series results) since this ratio coincides with C_+/C_- up to $O((6-d)^2)$ in the $(6-d)$ expansion.

d	Constant	This work	Previous work		γ/β
			Series	Monte Carlo	
2	β	0.13 ± 0.01	0.138 ± 0.007[a]	0.133 ± 0.010[b]	
	γ	2.48 ± 0.10	2.43 ± 0.03[a]	2.36 ± 0.10[b]	
	C_+/C_-	219 ± 25	$0(1)$[a]	196 ± 40[b]	17.6
3	β	0.42 ± 0.02	0.42 ± 0.06[c]	0.39 ± 0.02[d]	
	γ	1.78 ± 0.05	1.66 ± 0.07[c]	1.8 ± 0.05[d]	
	C_+/C_-	~ 8	...	11[b]	3.95
4	β	0.55 ± 0.05	0.52 ± 0.03[e]	0.52 ± 0.03[d]	
	γ	1.4 ± 0.1	1.41 ± 0.25[e]	1.6 ± 0.1[d]	
	C_+/C_-	~ 5	...	...	2.7
5	β	0.60 ± 0.08	0.66 ± 0.05[e]	0.66 ± 0.05[d]	
	γ	1.3 ± 0.1	1.25 ± 0.15[e]	1.3 ± 0.1[d]	
	C_+/C_-	~ 4	...	...	1.9
6	β	1.1 ± 0.2	0.97 ± 0.05[e]	0.97 ± 0.05[d]	
	γ	1.0 ± 0.1	1.06 ± 0.20[e]	1.0 ± 0.05[d]	
	C_+/C_-	~ 1	...	...	1
7	β	1.1 ± 0.2	...	...	
	γ	1.0 ± 0.1	...	...	
	C_+/C_-	...	...	...	1

[a]Reference 13. [c]Reference 14. [e]Reference 15.
[b]Reference 6. [d]Reference 7.

rizes the result of these operations in $d=2$ through 7. When the statistics are not excellent, however, the results depend heavily on which data points are covered by the least-squares fit. This consideration is the main source of the rather large error bars included in Table IV.

Figure 9 exhibits the two-, three-, and six-dimensional data for $P(p)$ and $\chi(p)$ together with the curves obtained by using the critical parameters (exponents and amplitudes) estimated as above. Clearly, both very close to p_c and far away from it, we expect deviations from the true critical behavior since, for the former, finite-size effects set in as soon as the connectedness length reaches the size of the sample, and as for the latter, since the critical region is exceeded. This figure is typical of our results in all dimensions, but we are not able to reproduce the corresponding figures for other dimensions because of the space considerations. Our results from $d=2$ and 3 are probably most reliable due to best statistics while those for $d=6$ are expected to be better than those for $d=7$, 4, or 5.

Among the remaining universal constants, the ratio of the critical amplitudes of the susceptibility, C_+/C_-, is of considerable interest. The $(4-d)$ expansion for the analogous quantity for the thermal Ising-like models[28] yields

$$C_+/C_- = 2^{\gamma-1}(\gamma/\beta) + O((4-d)^3) \quad . \tag{5.1a}$$

On the other hand, Aharony[29] recently showed for percolation,

$$C_+/C_- = 1 + \tfrac{2}{7}(6-d) + [565/(2)3^2 7^3](6-d)^2 + O((6-d)^3)$$
$$= \gamma/\beta + O((6-d)^3) \quad . \tag{5.1b}$$

This $(6-d)$ expansion provides the only theoretical estimate with which to compare our data, and therefore these are also included in Table IV. We note first that at $d=6$ this ratio from Eq. (5.1b), the mean-field approximation,[7,30] the Bethe lattice solution, and our Monte Carlo data are all consistent in giving the value unity. The convergence toward the mean-field results appears to be rapid, reinforcing our impressions gained in Sec. II.

At this point, we discuss our resolution of the controversy over the value of C_+/C_- for $d=2$. The series estimate was of order unity,[13] and our previous estimate[5] was about 20, where both of these were obtained from the mean cluster size function $S=\sum'_s s^2 n_s / \sum'_s s n_s$ ($\sum'$ implies summation omitting the infinite cluster). On the other hand, Hoshen *et al.*[6] used the susceptibility function $\chi=\sum'_s s^2 n_s$ to obtain $C_+/C_- \cong 200$. Since they also obtain 20 if the mean size function is used instead (albeit with unacceptably low exponent $\gamma=1.9$), the question is which function is to be used for scaling analysis. We have

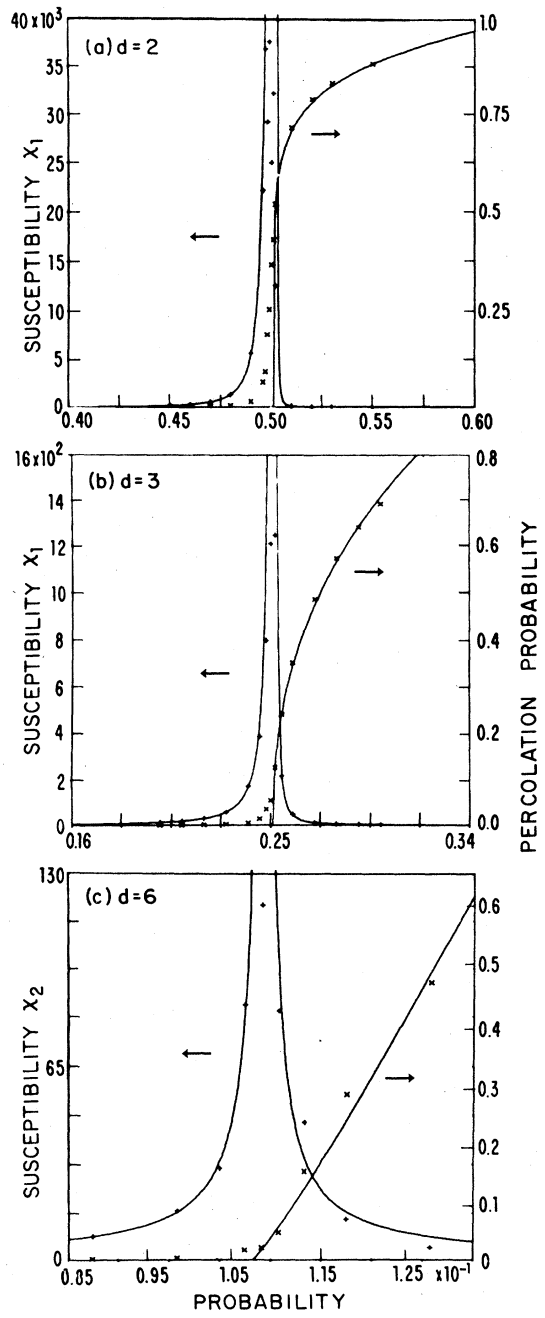

FIG. 9. Unscaled data for the percolation probability P (the fraction of sites in the largest cluster among the occupied sites) and susceptibility χ (the second moment of n_s) for (a) $d=2$, (b) $d=3$, and (c) $d=6$. The curves obtained from least-squares fitting the data linearly on log-log plots are also included. The rounding in P is a finite-size effect.

undertaken a thorough analysis of this point using our data in $d=2$ from lattices of three different sizes, as well as with two different ways (see below) to interpret the sum $\sum'$ appearing in S and χ in a finite system. Our finding is that χ must be used for at least two clear reasons: (1) When a suitable region

of p is selected to be fitted to a power law, setting $\gamma = \gamma'$ leads to results with an anomalous behavior in S for $p > p_c$ (upward curvature near p_c) while no such anomaly occurs in χ. This anomaly can be easily explained by the extra singularity introduced by the denominator in S [cf. Fig. 10(a)]. (2) The p_c^{eff} estimated from χ obeys a finite size scaling law (with a reasonable exponent $\nu \cong 1.5$) whereas that from S does not [cf. Fig. 10(b)].[31]

For these reasons, we have used χ in all dimensions. Actually, we used both χ_1 and χ_2 where in χ_1 we define $\sum'$ to mean the exclusion of the largest cluster for all p, and in χ_2 we take $\sum'$ to exclude the largest cluster only for $p > p_c^{\text{eff}}$. For $d = 2$ and 3, χ_1 and χ_2 give practically identical results whereas for $d \geq 4$ the results are substantially different. In particular, χ_1 tends to give unacceptably low values for the exponents γ and γ'. We attribute this to the rather severe effect of removing the largest cluster (below p_c) on a very small lattice. Also, although we use the individual n_s data, and *not* the grouped data as in Hoshen *et al.*[6] for $d = 2$, our estimate of $C_+/C_- \cong 219$ in $d = 2$ is very close to that of Hoshen *et al.*[6]

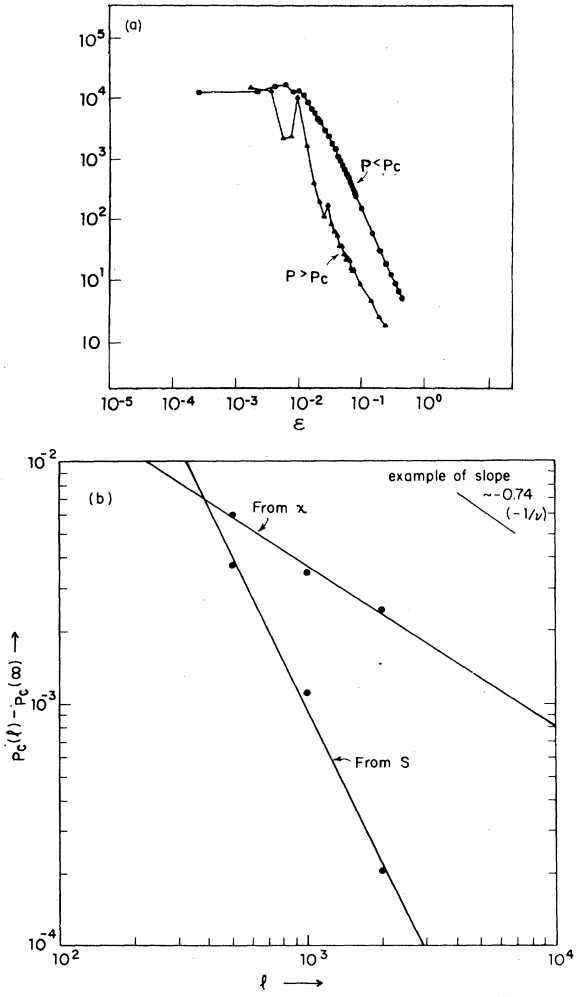

FIG. 10. Anomaly associated with the mean size function (susceptibility divided by the first moment) is shown; in (a), the upward curvature in the lower branch ($p > p_c$) represents the extra singularity in the denominator, and in (b) p_c^{eff} estimated from the susceptibility obeys the finite size scaling hypothesis well while that obtained from the mean size does not.

In three dimensions, our result of $C_+/C_- \cong 8$ differs considerably from Ref. 6 which gives 11 as their best estimate. Since both of our analyses use the individual n_s data here, the difference appears to be the lattice type and statistics. We have already pointed out that the bond problem tends to be "closer" to scaling than the site, and we have in general better statistics in $d = 3$. Indeed, fitting the regions $0.22 \leq p \leq 0.24$ and $0.26 \leq p \leq 0.28$ for the matching of γ and γ', the least-squares fit to the linear function in a log-log plot of χ vs $|p - p_c^{\text{eff}}|$ yields $R = 0.99998$ for $p < p_c^{\text{eff}}$ and 0.99999 for $p > p_c^{\text{eff}}$. Thus, we are inclined to believe that C_+/C_- is closer to 8 than to 11 (assuming universality, of course).

The results of $C_+/C_- \cong 1.0$ for $d = 6$ and $C_+/C_- \cong 2$ for $d = 7$ require some qualifications. In $d = 6$, if the region of p to be fitted were chosen to achieve best linearity in the log-log plot of χ vs $|p - p_c^{\text{eff}}|$, then we would find C_+/C_- to be as high as 2; however, the matched exponent thus obtained would be unacceptably high at 1.3. On the other hand, we may include data points closer to p_c in the fit, and this yields $\gamma = \gamma' = 1.0$ almost exactly, although with a somewhat worse correlation coefficient. This process also gives C_+/C_- of 1.0 almost exactly. Therefore, we consider this to be an evidence supporting the conjecture $C_+/C_- = 1$ although a larger value (perhaps as large as 2) could not be ruled out. A test of logarithmic correction to the susceptibility $\chi|\epsilon|^\gamma \sim |\ln|\epsilon||^\theta$ (with $\theta = \frac{2}{7}$) was also attempted, but the data scatter was too great to yield any tangible result. In $d = 7$, the estimate $C_+/C_- \cong 2$ seems to be barely compatible with $\gamma = \gamma' = 1$, which would imply the asymmetry of the scaling function about p_c appearing once again at $d = 7$. This would be highly anomalous since we expect C_+/C_- to remain unity once it achieves this value. However, this could be simply due to insufficient data and severe finite size effects as seen previously. The data for $p < p_c$ are particularly unreliable as already encountered in Sec. II.

The last universal constant we discuss here is the amplitude combination first studied by Stauffer,[32] for the bond or site problem, respectively,

$$K = C_+^{1/\delta} q_0^{-1} B^{1-1/\delta} \quad \text{(bond)}$$
$$= (C_+/p_c)^{1/\delta} (q_0/p_c)^{-1} B^{1-1/\delta} \quad \text{(site)} \ , \qquad (5.2)$$

where C_+ is the susceptibility amplitude for $p < p_c$ (C_- for $p > p_c$ could also be used), q_0 is the amplitude of the scaling function as studied in Sec. III, and B is the amplitude of the percolation probability [both C_+ and B are defined as the prefactors of the power-law term of $\epsilon = (p_c - p)/p_c$]. Stauffer[32] computed this constant in $d = 2$ from the extrapolation of the series results on the triangular site, square site, and honeycomb site problems, and obtained values ranging from 19 to 21. Our Monte Carlo results for the square bond problem corroborate this by yielding $K \cong 19$ or 20 where most of the uncertainty comes from that of q_0. Since this is the first result for a bond problem (as stated with q_0 in the definition of K), it is encouraging that the number is in good agreement with those of Stauffer for the site problem. In $d \geq 3$, there are no previous calculations of K, and since we have only one lattice type for each of $d = 3, \ldots, 7$, we are not able to state any conclusion about the universality of K. However, it may be useful to give our results on K for future reference. Thus, in $d = 3$, K is about 7 ± 1, and both in $d = 4$ and 5, it is about 6 ± 1. The results for $d = 6$ and 7 are much less certain, but in both of these dimensions, K is roughly 5 with the uncertainty of perhaps ± 2. The mean-field value for K is $2\sqrt{\pi} = 3.54 \ldots$. The $(6-d)$ expansion by Aharony[29] gives

$$K = \delta\Gamma(1 - 1/\delta)2^{1-2/\delta} + O((6-d)^3) \quad . \tag{5.3}$$

VI. CONCLUSIONS

In summary, we have, by extending the work of Hoshen *et al.*[6] beyond three dimensions, not only reaffirmed the scaling ansatz of Stauffer[4] but also found some new insights into the phenomenology of scaling in percolation. In two and three dimensions, we strengthen the previous findings; in higher dimensions we show that the trend established in $d \leq 3$ continues largely undisturbed except some key deviations such as the dominance of nonscaling terms in high d. Our results also focus on the important subject of what is and what is not universal. We find universal correction-to-scaling exponents for d up to 7; at the same time, the correction amplitude is shown quite clearly to be nonuniversal. We demonstrate numerically how the scaling functions change as functions of dimensionality. In particular, comparison between the Bethe lattice and $d = 6$, 7 are made and the asymmetry of Kunz-Souillard decay law[8] is conjectured to lie in the correction terms for $d \geq 6$. A correction to scaling consistent with a logarithmic correction is also seen at $d = 6$ for the first time for $n_s(p_c)$, the cluster number at p_c. In short, this paper strengthens the scaling approach in percolation in general, and at the same time presents interesting possibilities by supplying the first numerical results on many aspects of unresolved questions.

ACKNOWLEDGMENTS

First we benefitted greatly from the many discussions with and encouragement by Dr. D. Stauffer, Dr. J. Hoshen's expertise in computer programming was also essential since we reused the original two-dimensional data generated by the program written by him, and also since his concept of cluster multilabeling was applied by *HN* to three-dimensional percolation. (Our data for $d \geq 4$ were generated by an entirely different algorithm of breadth-first search.) We are also grateful to Drs. K Binder, G. Bishop, R. Harrison, C. Kawabata, W. Klein, S. Muto, S. Redner, and P. J. Reynolds for many useful discussions. Dr. A. Aharony is thanked for informing us of his recent work on $(6-d)$ expansions for percolation. The Academic Computing Center at Boston University kindly provided us with much needed computer time. This work was supported in part by ARO and AFOSR.

APPENDIX A

Here we discuss the details of the Monte Carlo simulations as well as some results, both analytic and numerical, pertaining to Sec. II which could not be accomodated there.

In two dimensions, we draw our data from the simulation of the bond problem on the square lattice. We performed 20 realizations at each of 80 values of p where $0.3 \leq p \leq 0.85$, for a lattice with $(500)^2 = 250\,000$ sites. Also, we performed 15 realizations at each of 64 values of p, where $0.275 \leq p \leq 0.7$, for a lattice with $(1000)^2 = 1\,000\,000$ sites, and 5 realizations at each of 16 values of p, where $0.45 \leq p \leq 0.55$, for a lattice with $(2000)^2 = 4\,000\,000$ sites or 8 million bonds. All of these simulations are done with free boundaries. The statistics of all the runs combined in $d = 2$ is roughly equivalent to Ref. 6. The data for n_s used in Sec. II and Appendix A are grouped in bins of $2^i \leq s < 2^{i+1}, i = 0, 1, 2, \ldots$ as in Ref. 6. As noted in Sec. I, the data points used for Eq. (2.6a) corresponds to $5 \leq i \leq 14$ or $2^5 \leq s < 2^{15}$.

Least-squares fit to Fig. 4(a) with a quadratic function yields

$$f((p_c - p)s^\sigma) = f(0)\exp(0.042 + 6.879x - 8.407x^2) \tag{A1a}$$

with the standard deviation $S = 1.277 \times 10^{-1}$ while the cubic fit gives

$$f((p_c - p)s^\sigma) = f(0)\exp(0.005 + 7.165x - 7.664x^2 - 1.102x^3) \tag{A1b}$$

with $S = 9.197 \times 10^{-2}$. These fits are extremely close

to the corresponding functions for the triangular site problem given by Ref. 6.

Our three-dimensional simulations are done for a simple cubic bond problem on a lattice with $(100)^3 = 1\,000\,000$ sites at each of 15 values of p, where $0.2 \leq p \leq 0.3$. Fifteen realizations are obtained for $0.2 \leq p \leq 0.248$, while 12 realizations are performed for $0.25 \leq p \leq 0.3$. Here also, we used the free boundary condition. The samples we use contain three million bonds, and thus we have three times the size of the lattice and at least as many concentrations as the principal samples which were used to obtain the scaling function for $d = 3$ in Ref. 6. Of course, their simulations were also done for different problems from ours (namely, the site problems on the simple cubic lattice and the bcc 1,2 lattice). Equation (2.6b) is obtained over the range $3 \leq i \leq 10$ or $2^3 \leq s < 2^{11}$ with $R = 0.99916$. In Fig. 4(b), the large scatter of the data points away from $x = 0$ is partly due to the fact that, because of the finite size of the lattice, this region can only be reached by taking a large ϵ, which takes us out of the scaling region. Another reason for this appears to be that, even within the scaling region, the finite size effect produces an oscillatory structure around the scaling function. This effect is seen in Sec. II also which will be discussed in Appendix B.

The quadratic fit to Fig. 4(b) yields

$$f((p_c - p)s^{\sigma}) = f(0)\exp(-0.014 + 2.646x - 9.191x^2) \quad \text{(A2a)}$$

with $S = 2.599 \times 10^{-1}$ while the cubic fit gives

$$f((p_c - p)s^{\sigma}) = f(0)\exp(-0.040 + 4.029x - 8.324x^2 - 5.62x^3) \quad \text{(A2b)}$$

with $S = 1.496 \times 10^{-1}$. Unfortunately, both fits miss the peak by a fair amount.

For $d = 4$, we performed for the site problem 20 realizations each at 6 values of p ($p = 0.177$, 0.187, 0.192, 0.197, 0.207, and 0.217) on the hypercubic lattice with $(20)^4 = 160\,000$ sites. These samples are generated with periodic boundaries. Although the scarcity of data makes it difficult to estimate the maxima of the n_s curves, a closer spacing would not make any sense for this size of samples since the pseudo-random-number generator we used would not produce the actual concentration of sites sufficiently close to the nominal concentration p. We also have a sample with $(40)^4 = 2\,560\,000$ sites; however, it is only generated at $p = 0.197$—the series estimate of p_c. Equation (2.6c) is obtained by fitting over the range $5 \leq i \leq 10$ or $2^5 \leq s < 2^{11}$. The scaling function of Fig. 4(c) is obtained by normalizing n_s by its value at $p = 0.197$ and using $\sigma = 0.493$ while our estimate of p_c best consistent with the susceptibility function is 0.198. Again we notice a large scatter of data points clustering around a roughly Gaussian curve on the semilog plot. The oscillatory nature of scatter strongly suggests the finite-size effects previously mentioned.

The best quadratic fit of Fig. 4(c) yields

$$f((p_c - p)s^{\sigma}) = f(0)\exp(0.024 + 2.891x - 15.899x^2) \quad \text{(A3a)}$$

with $S = 1.349 \times 10^{-1}$ while the best cubic fit gives

$$f((p_c - p)s^{\sigma}) = f(0)\exp(0.018 + 3.524x - 15.595x^2 - 7.881x^3) \quad \text{(A3b)}$$

with $S = 1.251 \times 10^{-1}$.

In five dimensions, our samples consist of 20 realizations each at 6 probabilities ($p = 0.121$, 0.131, 0.141, 0.146, 0.151, and 0.161) for the site problem on the hypercubic lattice with $(10)^5 = 100\,000$ sites. We also have one realization of 16^5 sample at $p = 0.141$, the series estimate of p_c. All of these are generated with periodic boundaries. The peaks of the functions $n_s(p)$ at several values of fixed s are too broad to estimate $p_{\max}$ with any precision; however, again the practical consideration of random number generation prevents us from spacing the data points more closely. Equation (2.6d) is obtained by fitting over the range $5 \leq i \leq 9$ or $2^5 \leq s < 2^{10}$.

The best quadratic fit to Fig. 4(d) is

$$f((p_c - p)s^{\sigma}) = f(0)\exp(-0.029 + 2.657x - 23.779x^2) \quad \text{(A4a)}$$

with $S = 7.428 \times 10^{-2}$ while the cubic fit gives

$$f((p_c - p)s^{\sigma}) = f(0)\exp(-0.028 + 2.822x - 23.799x^2 - 3.580x^3) \quad \text{(A4b)}$$

with $S = 7.424 \times 10^{-2}$. Again, the trend seen from $d = 1$, 2, 3, and 4 continues with no drastic change.

Since six dimensions is the upper marginal dimensionality for the percolation problem, we have conducted more thorough simulation for $d = 6$ and 7 than for $d = 4$ or 5. For $d = 6$, we simulate for the site problem 30 realizations of the hypercubic lattice with $(10)^6 = 1\,000\,000$ sites at each of 9 probabilities ($0.088 \leq p \leq 0.128$), all with periodic boundaries. For the sake of investigating some finite size effects, we have also generated 40 realizations of 5^6 lattice at various probabilities. The error bars indicated in Fig. 3(a) are nominal statistical ones estimated from dividing the total set of samples into three independent groups of 10 realizations at each probability and taking standard deviations.

As stated in Sec. II, we reject the possibility of the

breakdown of n_s scaling for $d=6$ in view of the rather good overall data collapse as seen in Fig. 4(e). To check that $p_c^{\text{eff}}=0.110$ is a more appropriate value here, we plotted $(p_c^{\text{eff}}-p_{\max})$ vs s for several trial values of $p_c \geq 0.108$ on a log-log scale. For $p_c^{\text{eff}}=0.108$, the resulting curve has a definite downward curvature, thus not reflecting any power laws. The choice of $p_c^{\text{eff}}=0.110$, on the other hand, results in a rather linear graph (presumably characterizing a power law correction to the logarithmically modulated scaling function). We have also simulated 5^6 samples to make certain that the finite size effect is responsible for the shift in p_c^{eff}. Among the 40 realizations generated at each of the probabilities between 0.103 and 0.113, 18 at $p=0.108$, and 23 at $p=0.110$ are actually used for this purpose (because of the deviations of the actual concentrations from the nominal ones). The result shows that $p_{\max}(s=362)$ is definitely greater than 0.108 just as for the case of 10^6 samples. Since this effect is in fact much more apparent in 5^6 case, we are led to the conclusion that this shift is mainly a finite size effect. The reason for our interpretation of the s dependence as corrections to scaling is essentially because we think that the scaling function is symmetric about p_c, and this point will be elaborated on in Sec. IV.

The best quadratic fit to Fig. 4(e) gives

$$f((p_c-p)s^{\sigma}) = f(0)\exp(-0.002+2.179x-41.076x^2) \quad \text{(A5a)}$$

with $S=1.047\times10^{-1}$ while the best cubic fit is

$$f((p_c-p)s^{\sigma}) = f(0)\exp(-0.010+2.685x-40.310x^2-13.267x^3) \quad \text{(A5b)}$$

with $S=1.011\times10^{-1}$.

For $d=7$, our Monte Carlo data are drawn from 16 realizations for the site problem on the hypercubic lattice with $(8)^7=2\,097\,150$ sites at each of 6 probabilities ($p=0.075$, 0.080, 0.085, 0.090, 0.095, and 0.100). Again, we use the periodic boundary condition.

In Sec. II, the backward "motion" of the peaks of the n_s curves (as s increases) was mentioned. We note here that this phenomenon is not related to the effect of finite s in the exact solution for the Bethe lattice. There, the use of Stirling's formula led to the symmetric scaling function (2.3), while if one uses (2.2) for finite s, one obtains $(p_c-p_{\max})\sim 2/[s(z-1)]$ (cf. Fig. 11). Thus, the leading correction to scaling makes $p_c > p_{\max}$, and never the other way as we see in $d=7$ results. In fact, we mentioned earlier that this sort of correction to scaling could account for the skewed appearance of f_6 as in Fig. 4(f).

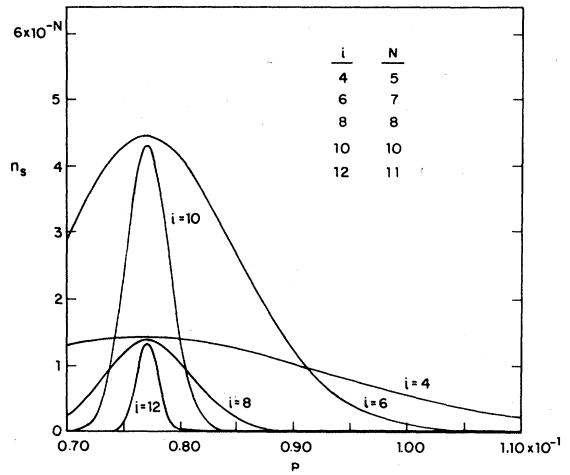

FIG. 11. Cluster size distribution for fixed s as function of p for the solution on the Bethe lattice with coordination number $z=14$. "i" indexes the bins for s.

The best quadratic fit to Fig. 4(f) gives

$$f((p_c-p)s^{\sigma}) = f(0)\exp(-0.033+0.918x-16.465x^2) \quad \text{(A6a)}$$

with $S=1.552\times10^{-1}$ while the best cubic fit yields

$$f((p_c-p)s^{\sigma}) = f(0)\exp(-0.040-0.642x-15.108x^2+34.542x^3) \quad \text{(A6b)}$$

with $S=1.139\times10^{-1}$.

APPENDIX B

In this appendix, we discuss the logarithmic correction to n_s for $d=6$ as stated in Eq. (3.16), as well as some details pertaining to Sec. III.

We begin with the question of the logarithmic correction. In terms of the cluster size distribution function, in analogy to the work of Rudnick and Nelson[33] for the thermal n-vector model, we postulate that, at p_c,

$$n_s \sim A\{1+[1-B/(\epsilon_d\Delta)](s^{-\epsilon_d\Delta}-1)\}^{\theta}s^{-\tau(\epsilon_d)}, \quad \text{(B1)}$$

where $\epsilon_d=6-d$ and A, B, Δ, θ are suitable values. [This is consistent with Eq. (3.8).] We shall determine Δ and θ as follows: (a) $\epsilon_d=6-d>0$, small. The expression in the bracket in Eq. (B1) can be written as

$$s^{-\epsilon_d}-[B/(\epsilon_d\Delta)](s^{-\epsilon_d}-1)\sim[B/(\epsilon_d\Delta)](1-s^{-\epsilon_d\Delta}) \quad \text{(B2)}$$

Since $1/s$ is taken to be very small, we have a

power-law correction to scaling

$$n_s \sim s^{-\tau(\epsilon_d)} + \text{const}\ s^{-\tau(\epsilon_d)-\epsilon_d\Delta} \ . \tag{B3}$$

Equations (3.8) and (3.13) then give

$$\epsilon_d\Delta = \omega\nu/\beta\delta = (1/4)\epsilon_d + O(\epsilon_d^2) \tag{B4a}$$

or

$$\Delta = 1/4 + O(\epsilon_d) \tag{B4b}$$

in ϵ_d expansion. (b) $\epsilon_d < 0$, small. Here, $1/s^{\epsilon_d\Delta}$ term in Eq. (B2) dominates, and we have, instead of a correction to scaling, scaling with a "different" exponent,

$$n_s \sim s^{-\epsilon_d\Delta\theta-\tau(\epsilon_d)} \ . \tag{B5}$$

Since above d_c, $n_s \sim s^{-2.5}$, we have $\epsilon_d\Delta\theta + \tau(\epsilon_d) \sim 2.5$, or

$$-\Delta\theta \sim [\tau(\epsilon_d) - 2.5]/\epsilon_d \ . \tag{B6}$$

Taking the limit $\epsilon_d \to 0-$, we obtain [assuming $\tau(\epsilon_d)$ to be smooth through $\epsilon_d = 0$],

$$\theta = -\tau'(\epsilon_d = 0)/\Delta [= -4\tau'(\epsilon_d = 0)] \ . \tag{B7}$$

(c) $\epsilon_d \to 0$. In this limit, we have

$$n_s \sim s^{-2.5}(\ln s)^{\theta} \ . \tag{B8}$$

Thus, the assumption (B1) leads to a logarithmic correction (B8) with $\theta = -4\tau'(0)$. We now use the fact that the ϵ_d-expansion results for the q-state Potts model (field theory) and in the limit $q \to 1$ is given by[34]

$$\beta = 1 - \tfrac{1}{7}\epsilon_d + O(\epsilon_d^2) \ ,$$

and

$$\gamma = 1 + \tfrac{1}{7}\epsilon_d + O(\epsilon_d^2) \ , \tag{B9a}$$

and thus

$$1/\delta = \tau - 2 = \tfrac{1}{2}[1 - \tfrac{1}{7}\epsilon_d + O(\epsilon_d^2)] \ . \tag{B9b}$$

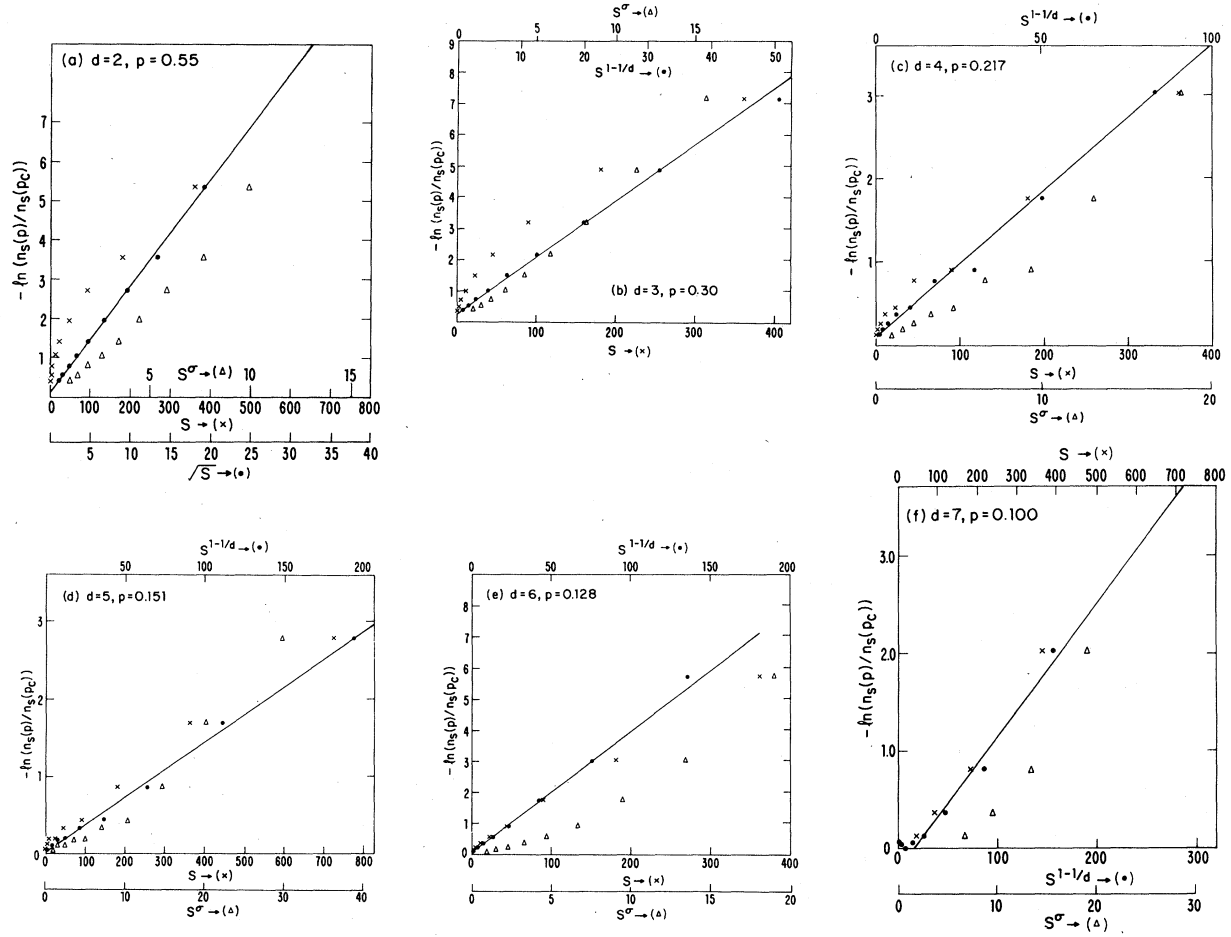

FIG. 12. Test of Kunz-Souillard decay law (4.1a) for (a) $d = 2$–(f) $d = 7$ by plotting $-\ln[n_s/n_s(p_c)]$ vs s, $s^{1-1/d}$, and s^{σ}.

Therefore, we finally obtain

$$\tau'(\epsilon_d = 0+) = \tau'(0) = -\frac{1}{14} \ , \tag{B10a}$$

leading to

$$\theta = \frac{2}{7} \ . \tag{B10b}$$

We note that this result is exact if Eq. (B1) is essentially correct. This is the scaling law with the logarithmic correction stated in Eq. (3.16).

For $d=2$, we note that the result from smaller lattices give very similar results to those with many millions of sites (such as those in Ref. 6). For example, $(1000)^2$ samples for the bond problem on the square lattice only requires us to look at a slightly smaller range of s, still yielding much the same results. Moreover, we generated just one realization at $p=0.5$ for the site problem on the triangular lattice with $(1000)^2$ sites, fully 16 times smaller than those used in Ref. 6, and still obtained more or less identical results to theirs, although finite size effects become apparent at a smaller value of s.

As to the oscillatory behavior mentioned in Sec. III, we find it to be a finite size effect by considering the data from three sizes of samples for the bond problem on the two-dimensional square lattice, $(500)^2$, $(1000)^2$, and $(2000)^2$. Whether we consider 5 realizations 10, or 20, we find this ripple starting from almost the same values of s (for each lattice size). For the three sizes these starting points are approximately 400, 1000, and 4000, respectively. We also note that these and other features of n_s (at p_c) are very insensitive to the size of the bin in which we group n_s data. Similar effect of "grouping" independence is also observed in the evaluation of χ (susceptibility) as will be described in Sec. V.

We note that, for the general analysis in $d=2$, we have used both the 15 samples of $(1000)^2$ and 5 of $(2000)^2$ at $p=p_c=0.5$, and for $d=3$, the 12 samples of $(100)^3$ at $p=0.250$. Similarly, for $d=4$ and 5, we have used 20 realizations of $(20)^4$ at $p=0.197$ and $(10)^5$ at $p=0.141$, respectively. Our one sample in $d=4$ of $(40)^4$ at $p=0.197$ corroborates the findings obtained using those of $(20)^4$. Similarly, the one sample of $(16)^5$ in $d=5$ supports the findings of Sec. III. For $d=6$, the 30 samples are of size $(10)^6$ and they are used at $p=0.110$; in seven dimensions, there are 16 samples of $(8)^7$ generated at $p=0.085$.

APPENDIX C

This appendix discusses the numerical results for Eq. (4.1) omitted in Sec. IV.

In Fig. 12(a), $-\ln[n_s(p=0.55)/n_s(p_c=0.5)]$ from our data for the two-dimensional square bond problem is plotted in three ways: vs s, $s^{1-1/d}=\sqrt{s}$, and s^{σ}. This plot, which is completely analogous to Fig. 8 of Ref. 6, clearly demonstrates Eq. (4.1a) for the square bond problem; the correlation coefficient R for linear fits of these points is 0.97053, 0.99873, and 0.99484 for s, $\sqrt{s}$, and s^{σ} in the abscissa, respectively. Figure 13(a), on the other hand, exhibits the same function vs $\sqrt{s}$ at several values of p in the range $0.51 \leq p \leq 0.7$. Although not shown, similar studies for values of p as close to p_c as 0.501

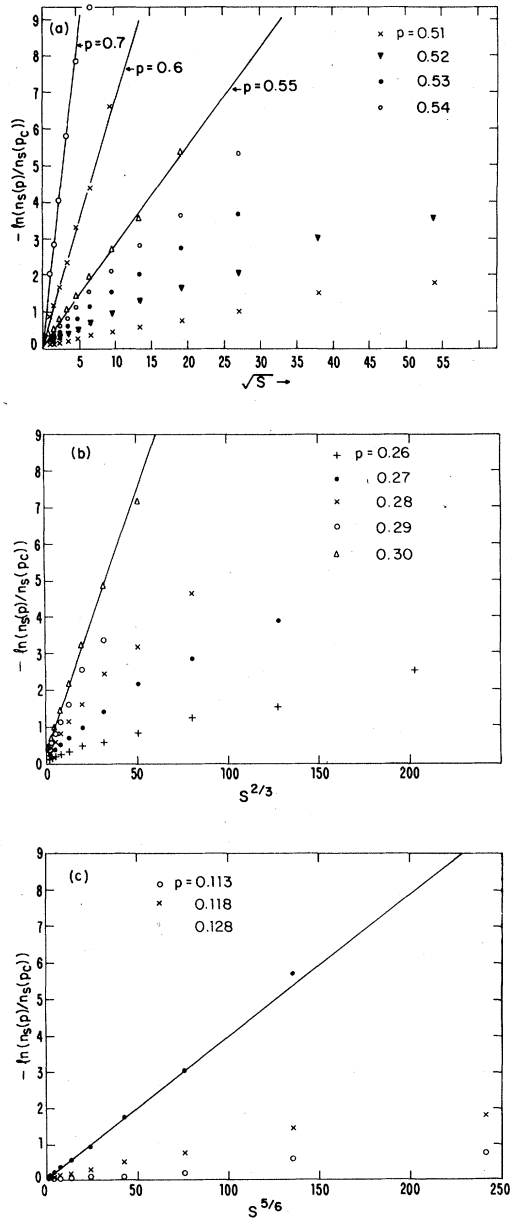

FIG. 13. Similarly to Fig. 12, $-\ln[n_s/n_s(p_c)]$ is plotted vs $s^{1-1/d}$ for (a) $d=2$, (b) $d=3$, and (c) $d=6$.

(2000 × 2000) and 0.505 (1000 × 1000) have also been made. The net result is that the Eq. (4.1a) seems to be valid only for $p \geq 0.54$ and not for smaller p. For example, at $p = 0.51$ (1000 × 1000), the linear fit vs s, $\sqrt{s}$, s^{σ} yields $R = 0.88991$, 0.98026, and 0.99288, respectively, over $0 \leq i \leq 14$, whereas at $p = 0.54$, $R = 0.95996$, 0.99891, and 0.99701 respectively over $0 \leq i \leq 9$. Although the closer to p_c, the larger the fluctuations, we believe that we are observing asymptotic behavior rather than a transient one because we have a rather large range of s for p close to p_c, different ranges of fit produce much the same result, and because R is in general reasonable indicating acceptable level of fluctuations. On the other hand, Eq. (4.1b) seems to be valid in a larger region. In Figs. 14(a)–14(c) plotted are $-\ln[n_s/n_s(p_c)]$ vs s for p in the range $0.275 \leq p \leq 0.495$ all showing the asymptotic behavior (4.1b) reasonably well. For example, even at $p = 0.49$, the linear fit to this function vs s, $\sqrt{s}$, s^{σ} yields $R = 0.99130$, 0.97426, and

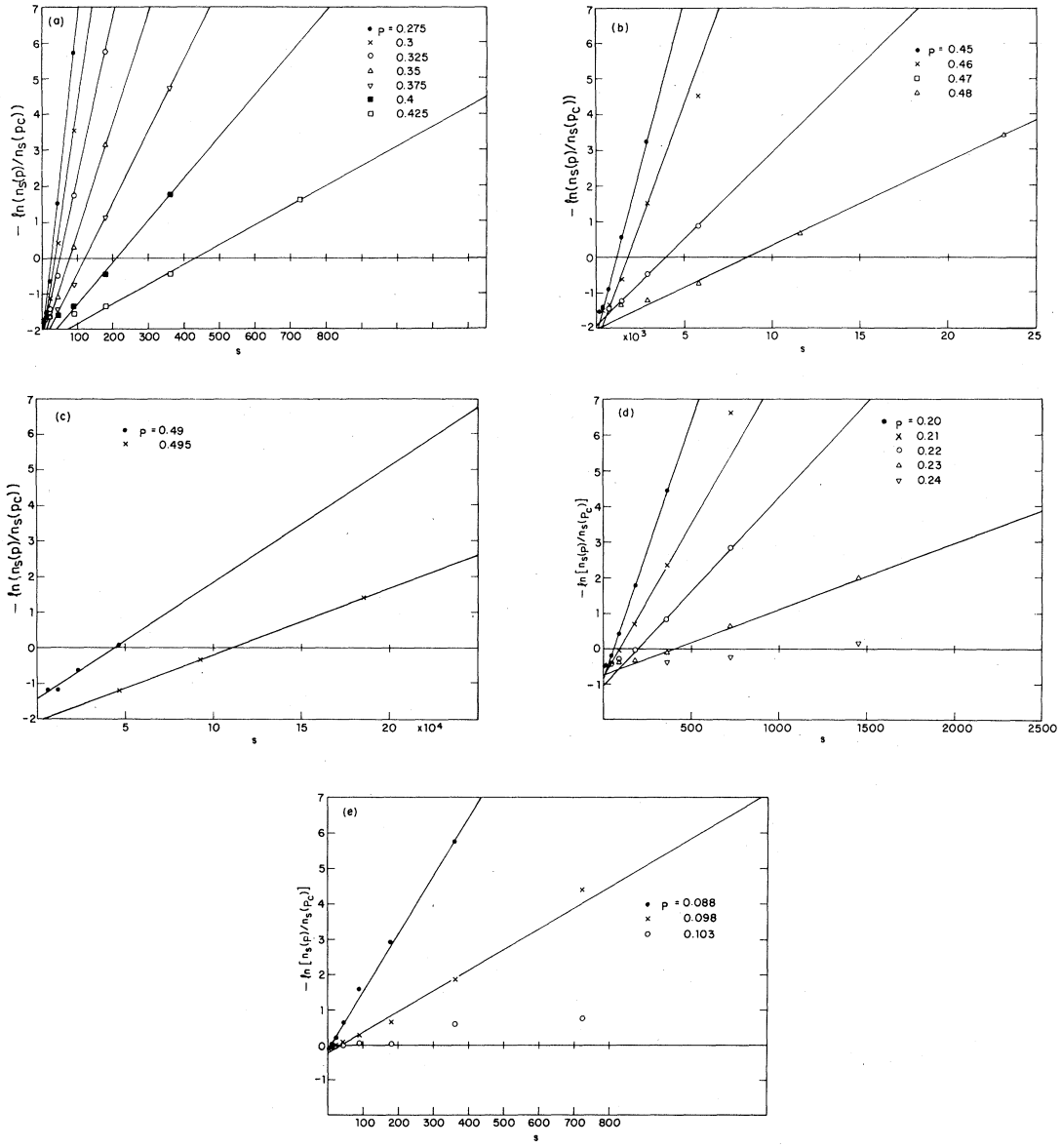

FIG. 14. Test of Kunz-Souillard decay law (4.1b) below p_c for (a)–(c) $d = 2$, (d) $d = 3$, and (e) $d = 6$ by plotting $-\ln[n_s/n_s(p_c)]$ vs s.

0.96713, respectively.

For $d=3$, the function $-\ln[n_s(p=0.3)/n_s(p=0.25)]$ is plotted in Fig. 12(b) vs s, vs $s^{1-1/d}=s^{2/3}$, and $s^{\sigma}=s^{0.47}$. Similarly to Fig. 12(a) for $d=2$, this plot demonstrates Eq. (4.1a) for the bond problem on the simple cubic lattice as $R=0.98529$, 0.99981, and 0.99542, respectively, over the range $0\leq i\leq 7$. Figure 13(b) is analogous to Fig. 13(a) for $d=2$, and it plots this function for p between 0.26 and 0.30. The values $p=0.252$ and 0.255 are also studied (not shown), but in these, the fluctuations are too large to permit quantitative analysis. For $0.26\leq p\leq 0.29$ we find linear fits vs $s^{2/3}$ is at best as good as those vs s^{σ} although considerably better than those vs s. For example, for $p=0.27$, $R=0.99009$ vs $s^{2/3}$ while $R=0.99881$ vs s^{σ} over the range $0\leq i\leq 10$. For $p<p_c$, we follow similar procedures, and obtain Figure 14(d) analogous to Fig. 13(b) for $p>p_c$. The linear fits vs s is much better than those vs $s^{2/3}$ in the case of $p>p_c$, and the region where these fits are unquestionably better is also larger, extending at least from 0.23 to 0.20 all with $R>0.999$.

In $d=4$, we have data at $p=0.207$, 0.217 above $p_c(=0.197)$ and 0.177, 0.187, and 0.192 below p_c. At $p=0.207$, $-\ln[n_s/n_s(p_c)]$ can be fitted to a straight line against $s^{1-1/d}=s^{3/4}$ and s almost equally well although much better than vs $s^{\sigma}=s^{0.493}$. At $p=0.217$, the fit vs $s^{3/4}$ is slightly better with $R=0.99598$ while it is 0.99513 and 0.97844 against s and s^{σ}, respectively, over $0\leq i\leq 8$ [Fig. 12(c)]. Below p_c, only $p=0.177$, the fit against s is clearly better than those vs $s^{3/4}$ or s^{σ} where $R=0.99517$, 0.98983, and 0.98178, respectively.

An analog of Figs. 12(a), (b), and (c) in $d=5$ is presented in Fig. 12(d) where linear fits to $-\ln[n_s(p=0.151)/n_s(p_c=0.141)]$ against s, $s^{1-1/d}=s^{4/5}$, and $s^{\sigma}=s^{0.515}$ yield $R=0.99589$, 0.99775, and 0.97788, respectively, over $0\leq i\leq 9$. Below p_c, both at $p=0.121$ and 0.131, linear fits are almost equally good (or bad) vs s, $s^{4/5}$, and $s^{0.515}$.

In six dimensions, the values $0.113\leq p\leq 0.128$ are used for $p>p_c(=0.110)$, but only 0.118 and 0.128 seem to yield clearly the Kunz-Souillard decay exponent of $1-1/d=5/6$. In Fig. 12(e) plotted is $-\ln[n_s(p=0.128)/n_s(p_c)]$ vs s, $s^{5/6}$, and $s^{\sigma}=\sqrt{s}$, resulting in $R=0.99904$, 0.99927, and 0.95774 respectively. Figure 13(c) is a similar plot for all $p>p_c$, while Fig. 14(e) is for $p<p_c$. For $p<p_c$, good fits vs s can be obtained only for $p\leq 0.098$.

Finally, for $d=7$, above $p_c=0.085$, for both $p=0.095$ and 0.1, the linear fit of $-\ln[n_s/n_s(p_c)]$ vs $s^{1-1/d}=s^{6/7}$ is equally good with those vs s whereas, for $p<p_c$, such fits are only possible at $p=0.075$. There, however, the fit against s appears to be better than those against $s^{6/7}$ or $s^{\sigma}=\sqrt{s}$. Figure 12(f) shows the same function at $p=0.1$ against s, $s^{6/7}$, and $\sqrt{s}$.

---

*This work forms a portion of the Ph.D thesis of H.N. to be submitted to the Dept. of Phys., Harvard University, Cambridge, Mass. 02138.

†Present address: Baker Laboratory, Cornell University, Ithaca, New York 14853.

[1]B. Widom, J. Chem. Phys. 43, 3892, 3898 (1965); C. Domb and D. L. Hunter, Proc. Phys. Soc. London 86, 1147 (1965).

[2]For a review, see K. G. Wilson and J. Kogut, Phys. Rep. 12, 75 (1974).

[3]P. W. Kasteleyn and C. M. Fortuin, J. Phys. Soc. Jpn. Suppl. 26, 11 (1969).

[4]The scaling hypothesis was first formulated for the percolation analogs of thermodynamic functions by J. W. Essam and K. M. Gwilym, J. Phys. C 4, L228 (1971), and for the cluster numbers by D. Stauffer, Phys. Rev. Lett. 35, 394 (1975).

[5]H. Nakanishi and H. E. Stanley, J. Phys. A 11, L189 (1978).

[6]J. Hoshen, D. Stauffer, G. H. Bishop, R. J. Harrison, and G. P. Quinn, J. Phys. A 12, 1285 (1979).

[7]Critical exponents and some percolation functions for d up to 6 are discussed using Monte Carlo techniques in S. Kirkpatrick, Phys. Rev. Lett. 36, 69 (1976).

[8]H. Kunz and B. Souillard, Phys. Rev. Lett. 40, 133 (1978); J. Stat. Phys. 19, 77 (1978).

[9]M. J. Stephen, Phys. Rev. B 15, 5674 (1977); M. R. Giri, M. J. Stephen, and G. S. Grest, *ibid.* 16, 4971 (1977). See also J. W. Essam, D. S. Gaunt, and A. J. Guttmann, J. Phys. A 11, 1983 (1978) for the renormalization-group and series analyses of the logarithmic corrections to scaling at $d=6$.

[10]A. Hankey and H. E. Stanley, Phys. Rev. B 6, 3515 (1972).

[11]P. J. Reynolds, H. E. Stanley, and W. Klein, J. Phys. A 10, L203 (1977); D. Stauffer and C. Jayaprakash, Phys. Lett. 64A, 433 (1978).

[12]M. E. Fisher and J. W. Essam, J. Math. Phys. 2, 609 (1961).

[13]Series estimates of σ are obtained using $\sigma=1/(\beta\delta)=(\beta+\gamma)^{-1}$. In two dimensions β and γ are estimated in M. F. Sykes, D. S. Gaunt, and M. Glen, J. Phys. A 9, 97, 725 (1976).

[14]M. F. Sykes, D. S. Gaunt, and J. W. Essam, J. Phys. A 9, L43 (1976); and M. F. Sykes, D. S. Gaunt, and M. Glen, J. Phys. A 9, 1705 (1976).

[15]D. S. Gaunt, M. F. Sykes, and H. Ruskin, J. Phys. A 9, 1899 (1976); similar studies are done in D. S. Gaunt and H. Ruskin, J. Phys. A 11, 136 (1978) for the hypercubic bond problem.

[16]R. K. P. Zia and D. J. Wallace, J. Phys. A 8, 1495 (1975); D. J. Amit, D. J. Wallace, and R. K. P. Zia, Phys. Rev. B 15, 4657 (1977).

[17]P. L. Leath and G. R. Reich, J. Phys. C 11, 4017 (1976).

[18]V. K. S. Shante and S. Kirkpatrick, Adv. Phys. 20, 325 (1971).

[19]D. S. Gaunt and M. F. Sykes, J. Phys. A 9, 1109 (1976) for $d=2$, and D. S. Gaunt, J. Phys. A 807 (1977) for $d=3$.

[20]F. J. Wegner, Festkorperprobleme 16, 1 (1976) developed this idea in the context of renormalization group.

[21]A. Houghton, J. S. Reeve, and D. J. Wallace, Phys. Rev. B 17, 2956 (1978). See also Amit, Wallace, and Zia (Ref. 16).

[22]F. J. Wegner and E. K. Riedel, Phys. Rev. B 7, 248 (1973).

[23]A. Sur, J. L. Lebowitz, J. Marro, M. H. Kalos, and S. Kirkpatrick, J. Stat. Phys. 15, 345 (1976).

[24]M. M. Bakri and D. Stauffer, Phys. Rev. B 14, 4215 (1976).

[25]W. Klein and D. Stauffer (unpublished); also, see F. Delyon (unpublished).

[26]J. Hoshen *et al.* (Ref. 6); E. Stoll and C. Domb, J. Phys. A 11, L57 (1978); W. Kinzel, Z. Phys. B 34, 79 (1979).

[27]The Bethe lattice (or $d=\infty$) leads to the symmetric decay and thus the scaling term could again be dominant. In thermal Ising-like systems, decay laws similar to the Kunz-Souillard results are valid [F. Delyon, J. Stat. Phys. (in press)]. There, C_+/C_- (isothermal magnetic susceptibility amplitude ratio) is 2 for all $d \geq 4$. Therefore, the scaling term cannot dominate in the Bethe lattice solution in that case.

[28]E. Brézin, J. C. Le Gillou, and J. Zinn-Justin, in *Phase Transitions and Critical Phenomena*, edited by C. Domb and M. S. Green (Academic, London, 1976), Vol. 6.

[29]A. Aharony, Phys. Rev. B (in press).

[30]L. Mittag and M. J. Stephen, J. Phys. A 7, L109 (1974).

[31]We have also analyzed in the same way the Monte Carlo data of Dean and Bird [P. Dean and N. F. Bird, National Physical Laboratory Report Ma61, Teddington, England (1966) (unpublished)] for the bond problem on the lattice with 62500 bonds. The result is that the difference between χ and S as described in (1) can still be seen while the finite size scaling analysis of (2) cannot be extended to this size. This is because they used bond counting and also because the finite size effects are so severe that there is no extended region of p that could be fitted to a single power law.

[32]D. Stauffer, Z. Phys. B 25, 391 (1976); J. Marro, Phys. Lett. 59A, 180 (1976).

[33]J. Rudnick and D. R. Nelson, Phys. Rev. B 13, 2208 (1976).

[34]D. J. Amit, J. Phys. A 9, 1441 (1976); R. G. Priest and T. C. Lubensky, Phys. Rev. B 13, 4159 (1976); 14, 5126(E) (1976).

[35]E. Jahnke, F. Emde, and F. Lösch, *Tables of Higher Functions* (McGraw-Hill, New York, 1960).